

Confining dyon-antidyon Coulomb liquid model. I.Yizhuang Liu,^{*} Edward Shuryak,[†] and Ismail Zahed[‡]*Department of Physics and Astronomy, Stony Brook University, Stony Brook, New York 11794-3800, USA*

(Received 4 May 2015; published 5 October 2015)

We revisit the dyon-antidyon liquid model for the Yang-Mills confining vacuum discussed by Diakonov and Petrov, by retaining the effects of the classical interactions mediated by the streamline between the dyons and antidyons. In the SU(2) case the model describes a 4-component strongly interacting Coulomb liquid in the center symmetric phase. We show that in the linearized screening approximation, the streamline interactions yield Debye-Huckel-type corrections to the bulk parameters, such as the pressure and densities, but do not alter significantly the large-distance behavior of the correlation functions in leading order. The static scalar and charged structure factors are consistent with a plasma of a dyon-antidyon liquid with a Coulomb parameter $\Gamma_{D\bar{D}} \approx 1$ in the dyon-antidyon channel. Heavy quarks are still linearly confined and the large spatial Wilson loops still exhibit area laws in leading order. The t' Hooft loop is shown to be one modulo Coulomb corrections.

DOI: 10.1103/PhysRevD.92.085006

PACS numbers: 11.15.Kc, 11.30.Rd, 12.38.Lg

I. INTRODUCTION

At asymptotically high temperature T , QCD-like theories are in a weakly coupled state known as the quark-gluon plasma (QGP). In this state, semiclassical solitons— instantons and their constituents, monopoles, etc.—have large action $S = O(1/\alpha_s) \gg 1$. Their semiclassical treatment is parametrically reliable in such a limit, yet their density is exponentially small $\sim e^{-S}$ and their effects are small.

However, as the temperature decreases the semiclassical action S decreases. Since the soliton density grows as a power of $1/T$, their contribution to the QCD partition increases. At some critical density fixed by T_c , confinement sets in, and the near-zero expectation value of the Polyakov line $\langle L \rangle \approx 0$ switches off the quark component of the QGP, as well as the (nondiagonal) gluons. Below the critical temperature T_c , the solitons dominate the field ensemble.

The major questions at the transition point are the following: (i) Are these objects still made of strong enough fields, allowing for a semiclassical analysis? (ii) Are their interactions weak enough to preserve their individual identity? (iii) Are the semiclassical interactions in the thermal ensemble amenable to known methods of many-body theory? As we will argue below, the first two questions will be answered in the affirmative, and the third, also, provided the ensemble is dense enough.

The instanton liquid model developed in the 1980s is an example of such a semiclassical treatment. In the vacuum at $T = 0$, the action per typical SU(3) instanton was found to be large with $S \sim 12$, and the interinstanton and anti-instanton interactions were found to be tractable. The

nonperturbative vacuum topological fluctuations are related to the explicit violation of the axial U(1) and the formation of fermionic zero modes. The collectivization of the fermionic zero modes leads to the spontaneous breaking of flavor chiral symmetry [1] (and references therein). More recently, instanton-induced effects were found to be important for hadronic spin physics [2].

However, around the critical temperature $T \sim T_c$, instantons should know about the nonvanishing of the Polyakov line expectation value, also referred to as a nontrivial holonomy. Instantons with nontrivial holonomies were found by Lee-Li-Kraan-van Baal (LLKvB) in [3]. The key discovery was the realization that nonzero holonomies split instantons into N_c constituents, the selfdual instanton-dyons. Since these objects have nonzero (Euclidean) electric and magnetic charges and source Abelian (diagonal) massless gluons, the corresponding ensemble is an “instanton-dyon plasma.”

Diakonov and Petrov [4] emphasized that, unlike the (topologically protected) instantons, the dyons interact directly with the holonomy field. They further suggested that since such dyon (antidyon) fields become significant at low temperature, they may be at the origin of a vanishing of the mean Polyakov line, or confinement. This mechanism is similar to the Berezinsky-Kosterlitz-Thouless-like transition of instantons into fractional “instanton quarks” suggested earlier by Zhitnitsky and others [6], inspired by the fractionalization of the topological charge in two-dimensional CPN models [7], although it is substantially different in detail. It is also different from the random dyon-antidyon ensemble suggested earlier by Simonov and others [8]. It is not yet clear how this Euclidean mechanism relates to the quantum condensation of magnetic monopoles suggested initially by t' Hooft [9] and Mandelstam [10], and subsequently supported in the supersymmetric model discussed by Seiberg and Witten

^{*}yizhuang.liu@stonybrook.edu[†]edward.shuryak@stonybrook.edu[‡]ismail.zahed@stonybrook.edu

[11]. In many ways, it is similar to the three-dimensional monopole plasma discussed by Polyakov [12].

Unsal and Yaffe [13], using a double-trace deformation of Yang-Mills at large N on $S^1 \times R^3$, argued that it prevents the spontaneous breaking of center symmetry. A similar trace deformation was used in the context of two-dimensional (confining) QED with unequal charges on $S^1 \times R$ [14] to analyze the nature of center symmetry and its spontaneous breaking. This construction was extended to QCD with adjoint fermions by Unsal [15], and by Unsal and others [16] to a class of deformed supersymmetric theories with soft supersymmetry breaking. While the setting includes a compactification on a small circle, with weak coupling and an exponentially *small* density of dyons, the minimum at the confining holonomy value is induced by the repulsive interaction in the dyon-antidyon pairs (called *bions* by the authors). The supersymmetry is needed to calculate the contribution of the dyon-antidyon pairs, and, even more importantly, for the cancellation of the perturbative Gross-Pisarski-Yaffe-Weiss (GPYW) holonomy potential [17].

Shuryak and Sulejmanpasic [18] have argued that induced by the “repulsive cores” in dyon-antidyon channel also generate confinement, explaining it in a simple model. The first numerical study of the classical interaction of the dyons with antidyons has been recently carried in [22]. The streamline configurations were found by a gradient flow method, and their action assessed. This classical interaction will be included—for the first time—in our paper.

Another major nonperturbative phenomenon in QCD-like theories is spontaneous chiral symmetry breaking. Shuryak and Sulejmanpasic [19] have analyzed a number of phenomena induced by the fermionic zero modes of the instanton-dyons such as the formation of clusters (molecules or bions) at high temperature and their collectivization, generating spontaneous breaking of chiral symmetry at low temperature. Faccioli and Shuryak [20] have started numerical simulations of the dyon ensemble with light fermions to understand the nature of the fermionic collectivization. We will provide an analytical analysis of these effects in the second paper of this series.

Before we get into the details of the various approximations to our analysis, let us try to provide some qualitative answers to the three generic questions formulated above: (i) At $T \sim T_c$, we will consider the action per dyon (antidyon) to be still large or $S \sim 4$ whatever N_c ; (ii) The dyon interactions will be of the order of $\Delta S_{\text{int}} \sim 1 \ll S$. The quantum (one-loop) interactions are several times smaller and naively can be considered small. However they are quite nontrivial and the repulsion they provide would be our key finding. (iii) In general, the dyon plasma is strongly coupled and it is hard to treat it analytically. However we will argue below that in some window of temperatures (below T_c) one can still use the Debye-Huckel plasma theory.

A major contribution to the understanding of the one-loop dyon interaction has been made by Diakonov and others [4,5]. They have found that at $T > T_c$ their interaction with the surrounding QGP leads to a linear (confining) potential between the dyons, proportional to the perturbative Debye mass. Since in this work we will only consider the opposite case $T < T_c$, this will not be included in what follows. Key to the one-loop effect is the explicit quantum weight of the KvBLL instantons in terms of the collective coordinates of the constitutive dyons at all separations. The self-dual sector is characterized by a moduli space with a hyper-Kähler metric. Its volume element is given by the determinant of Coulomb-like matrix. We will refer to it as Diakonov determinant.

In his first attempts to treat the dyonic plasma, Diakonov kept only the one loop determinant, the volume of the moduli space, ignoring the QGP screening effects and—as we will discuss in detail—the even larger classical dyon-antidyon interaction. Furthermore, he assumed that the attractive and repulsive terms induced by the determinant cancel out on average. We disagree on this conclusion as we detail below. Indeed, Bruckmann and others in [21] tried to generate configurations of randomly placed dyons using the determinantal measure, and observed that for the physically relevant dyonic densities, the determinantal measure develops negative eigenvalues. This makes no sense if the measure is to account for the volume of the dyonic moduli space. We will show that this issue may become resolved in a strongly correlated ensemble.

It is well known that the separate treatment of self dual and anti-selfdual sectors is only justified in the context of supersymmetry where self-duality is dual to holomorphy. In QCD-like theories, the interaction between self dual and anti-selfdual sectors is strong and not factorizable. It is described semiclassically by a “streamline” with a classical inter-particle potential of order $1/\alpha_s$, which is larger than the 1-loop quantum induced potential of order α_s^0 . Furthermore, configurations with too strongly overlapping objects with small action, are not subject to the semiclassical treatment. To account for that one usually relies on the use of a “repulsive core” as in the instanton liquid model for instance.

As we will discuss in detail, classical dyon-antidyon interaction [22] is about an order of magnitude stronger than the one-loop Coulomb effects. It generically leads to the dyon plasma in the strongly coupled regime, with $e^{-V_{db}} \gg 1$. We will however focus on the very dense regime of such plasma, in which screening is strong enough that statistical mechanics of the ensemble can be treated by a variant of the Debye-Huckel mean field plasma theory. In such case the screening length is short enough to fence the system from strong coupling correlations and molecular-type instabilities induced by the streamline. The more dilute systems such as those appearing at $T > T_c$, will not be discussed in this work, as they need more powerful

many-body methods, such as e.g. strongly coupled Coulomb plasmas many-body physics re-summations [23,24] (and references therein). As we will show, in this case the free energy has a minimum at the “confining” holonomy value $v = \pi T$.

In this paper we will detail the strongly coupled nature of the dyonic plasma. Our original results consist of (i) introducing the strong correlations between dyons and antidyons as described by the streamline [22], (ii) showing that the determinant interactions induced by the moduli space for dyons or antidyons are mostly repulsive causing the moduli volume to vanish for randomly distributed dyons, (iii) showing that suitably organized dyons, in order to account for screening correlations, yield finite moduli volumes; (iv) deriving an explicit three-dimensional effective action that accounts exactly for the screening of dyons and antidyons on the moduli space with strong inter-dyon-antidyon streamline interactions, (v) showing explicitly that the strongly coupled dyonic plasma is center symmetric and thus confining, (vi) deriving the Debye-Huckel corrections induced by the dyons and antidyons to the leading pressure for the dyonic plasma and using it to assess the critical temperature for the SU(2) plasma, (vi) providing the explicit results for the gluon topological susceptibility and compressibility near the critical temperature in the center symmetric phase, (vii) deriving the scalar and charged structure factors of the dyonic plasma showing explicit screening of both electric and magnetic charges at large distances with explicit predictions for the electric and magnetic masses, and (viii) showing that the strongly coupled dyonic plasma supports both electric and magnetic confinement.

This paper is organized as follows: In Sec. II we review the key elements of the dyon and antidyon measure derived in [4,5] using the KvBLL instanton. The dyon-antidyon measure is then composed of the product of two measures with streamline interactions between the dyons and antidyons. We briefly detail the exact rewriting of the three-dimensional grand-partition function in terms of a three-dimensional effective theory in the SU(2) case. We also show that the ground state of this effective theory is center symmetric. In Secs. III and VI we show that in the linearized screening approximation, the dyon-antidyon liquid still screens both electric and magnetic charges, generates a linearly rising potential between heavy charges, and confines the large spatial Wilson loops. The t' Hooft loop in the dyon-antidyon ensemble is shown to be 1 modulo $\mathcal{O}(\alpha_s)$ self-energy corrections which are perimeter-like in Sec. VII. Our conclusions are in Sec. VIII.

II. INTERACTING DYON-ANTIDYON ENSEMBLE

A. The setting

The first step is the introduction of the nonzero expectation value of the fourth component of the gauge field,

which is gauge invariant since at finite temperature it enters the holonomy integral over the time period, known also as the Polyakov line. Working in a gauge in which $\langle A_4 \rangle$ belongs to the diagonal and traceless subalgebra of $N_c - 1$ elements, one observes the standard Higgsing via the adjoint field. All gluons except the diagonal ones become massive. We will work with the simplest case of two color gauge theory $N_c = 2$, in which there is only one diagonal matrix and the VEV of the gauge field (holonomy) is normalized as follows,

$$\langle A_4^3 \rangle = v \frac{\tau^3}{2} = 2\pi T \nu \frac{\tau^3}{2}, \quad (1)$$

where $\tau^3/2$ is the only diagonal color generator of SU(2). At high T it is trivial with $\nu \rightarrow 0$, and at low $T < T_c$ it takes the confining value $\nu = 1/2$. With this definition, the only dimensional quantity in the classical approximation is the temperature T , while the quantum effects add to the running coupling and its Λ parameter. Since we are working near and below T_c , we follow the lattice practice and use the latter as our main unit.

In the semiclassical approximation, the Yang-Mills partition function is assumed to be dominated by an interacting ensemble of dyons (antidyons) [4,5]. For large separations or a very dilute ensemble, the semiclassical interactions are mostly Coulombic and are encoded in the collective or moduli space of the ensemble. For multidyons a plausible moduli space was argued starting from the KvBLL caloron [3] that has a number of pertinent symmetries, including permutation symmetry, overall charge neutrality, and clustering to KvBLL at high temperature. Since the underlying calorons are self-dual, the induced metric on the moduli space was shown to be hyper-Kähler.

The SU(2) KvBLL instanton (anti-instanton) is composed of a pair of dyons labeled by L, M (antidyons by \bar{L}, \bar{M}) in the notations of [4] which we will follow. Unsal and collaborators use another name for them: $L = \text{KK}$ and $M = \text{BPS}$, rooted in historical development. BPS stands for Bogomolny-Prasad-Sommerfeld original monopole solution and KK stands for Kaluza-Klein or “time-twisted” solution. Their actions are $S_L = 2\pi v_m / \alpha_s$ and $S_M = 2\pi v_l / \alpha_s$. The M dyons carry $(+, +)$ and L carries $(-, -)$ (Euclidean electric-magnetic) charges according to the massless diagonal gluons.

Let us remark on the terminology and the nature of the electric charges and fields we use: those are real in the Euclidean spacetime setting, and for the solitons used they are, up to possibly a sign, the same as the magnetic ones at any point. Both the electric and magnetic charges of the instanton-dyons are observable by standard Gaussian closed surface fluxes. If one tried to return to Minkowski spacetime, however, these electric fields would become imaginary, while the magnetic ones would remain real.

One may also recall that the M dyon is indeed nothing but the original BPS monopole solution of the Georgi-Glashow model, with the adjoint Higgs scalar substituted by the component of the gauge field $\phi \rightarrow A_4$. After this substitution, however, gradients $\nabla\phi \rightarrow \nabla A_4$ and are called the electric field; the solution is self-dual. No longer a solution in the Georgi-Glashow model, it now belongs to pure gauge theory at nonzero holonomy.

Unsal and collaborators call these objects instanton-monopoles, arguing that the electric charges or fields are unlike magnetic ones since they are “not real.” We do not see how this distinction can possibly be relevant since the notion of a nonzero holonomy itself, the idea of instantons or instanton-dyons as the saddle points of the path integrals and many more parts of the setting used, does not exist outside of the Euclidean finite- T formulation. Anyway, it is just the names, since all expressions used are the same.

For clarity, let us also comment that these Euclidean objects are not, by any means, the particle-monopoles, the excitations of the theory, which must exist in Minkowski spacetime. Those are not even known for pure gauge theory.

The statistical measure for a correlated ensemble of dyons and antidyons is

$$d\mu_{D\bar{D}}[K] \equiv e^{-V_{D\bar{D}}(x-y)} \prod_{m=1}^N \prod_{i=1}^{K_m} \frac{f d^3 x_{mi}}{K_m!} \det(G_{mi}[x]) \times \prod_{n=1}^N \prod_{j=1}^{\bar{K}_n} \frac{f d^3 y_{nj}}{\bar{K}_n!} \det(G_{nj}[y]). \quad (2)$$

The streamline interactions induced by the potential $V_{D\bar{D}}$ correlate the two otherwise statistically independent dyon and antidyon sectors. (Note that by the potential we mean the extra action and not the energy; thus, no extra $1/T$). Asymptotically,

$$V_{D\bar{D}}(x-y) \rightarrow \sum_{mn,ij} \frac{C_D/2}{\alpha_s T} \frac{Q_{mi} \bar{Q}_{nj}}{|x_{mi} - y_{nj}|} \quad (3)$$

is a Coulomb-like classical interaction between dyons and antidyons. Here x_{mi} and y_{nj} are the three-dimensional coordinates of the i dyon of the m kind and the j antidyon of the n kind. At shorter separations the streamline stops at a certain distance $a_{D\bar{D}}$, and we will refer to it as the “core size.” While the interaction is more complex than just the electric Coulomb, it is proportional to the electric charges Q, \bar{Q} . In general, those are the (Cartan) roots of $SU(N_c)$ supplemented by the affine root. They satisfy

$$Q_{mi} \bar{Q}_{nj} \equiv -(2\delta_{mn} - \delta_{m,n+1} - \delta_{m,n-1}). \quad (4)$$

The dimensionality of $G[x]$ is $(K_1 + \dots + K_N)^2$ and similarly for $G[y]$. Their explicit form can be found in [4,5]. In the $SU(2)$ case there is only one electric charge.

The semiclassical 3-density of all dyon species $n_D \equiv n_L + n_M + n_{\bar{L}} + n_{\bar{M}}$ is

$$n_D = \frac{dN}{d^3x} = \frac{CT^3 e^{-\frac{\pi}{\alpha_s}}}{\alpha_s^2}, \quad (5)$$

where C is a constant to be determined below [see (56)]. Equation (5) can be rewritten using the asymptotic freedom formula for $SU(2)$ pure gauge theory with $2\pi/\alpha_s(T) = (22/3) \ln(T/\Lambda)$ in terms of the scale parameter Λ . (Strictly speaking, $22/3$ should be 8 since we are ignoring the effects of nonzero modes). The dimensionless density

$$\frac{n_D}{T^3} \sim \left(\frac{\Lambda}{T}\right)^{11/3} \quad (6)$$

is small at high T but increases as T decreases. With the exception of Sec. III G, where we will estimate the critical deconfinement temperature by including perturbative $\mathcal{O}(\alpha_s^0)$ effects in the dimensionless pressure, we will always assume the temperature to be small enough, so that the dyon effects are the dominant ones. The dyon fugacity f is

$$f \approx \frac{n_D}{8\pi} \quad (7)$$

to order $\mathcal{O}(n_D^{3/2})$ in the dyon density (see below). The absolute value of the parameter Λ appearing in the semiclassical formulas can be related to standard parameters like $\Lambda_{\overline{\text{MS}}}$, but this has no practical value since the accuracy with which they are known is too low to give an accurate value of the dyonic density. In practice it is obtained from the fit to the lattice instanton data performed in [19] in the range $0.5 < T/T_c < 3$. The caloron action—the sum of S_L and S_M —is then written as

$$S_{L+M}(T) \equiv \frac{2\pi}{\alpha_s(T)} \equiv \frac{22}{3} \ln\left(\frac{T}{0.36T_c}\right). \quad (8)$$

We will use this fit as a basis for our running coupling. In particular, the action of the $SU(2)$ caloron at T_c $S_{L+M}(T_c) \approx 7.47$ translates to the value of the coupling $\alpha_s(T_c) = 0.84$. Since in this paper we only work in the confining regime of the holonomy with all dyon actions identical, the action per dyon is about 3.75.

The repulsive linear interaction between unlike dyons (antidyons) found in [5] acts as a linearly confining force in the center asymmetric phase, favoring the molecular or KvBLL configuration at $T > T_c$. This interaction stems from QGP thermal quanta scattering on the dyons. However, we will be interested in this paper in the center symmetric phase at $T < T_c$, in which there is no QGP, and we do not include this interaction.

Since the classical $V_{D\bar{D}} \sim 1/\alpha_s$, it dominates the quantum determinants, which include Coulomb interaction of order α_s^0 . On this point we differ from the argument presented in [4] regarding the reorganization of (3) in an extended quantum determinant. At large relative separations between all particles, the measure (3) is exact. It is also exact when each bunch of dyons or antidyons coalesces into a KvBLL instanton or anti-instanton at all separations.

The above notwithstanding, the grand-partition function associated with the measure (3),

$$\mathcal{Z}_{D\bar{D}}[T] \equiv \sum_{[K]} \int d\mu_{D\bar{D}}[K], \quad (9)$$

describes a highly correlated ensemble of dyon-antidyons which is no longer integrable in the presence of the streamline. The case $V_{D\bar{D}}=0$ amounts to $\mathcal{Z}_{D\bar{D}} \rightarrow \mathcal{Z}_D \mathcal{Z}_{\bar{D}}$, where each factor can be exactly rewritten in terms of a three-dimensional effective theory. We now analyze (9) for the SU(2) case, following and correcting the arguments in [4],

$$\begin{aligned} \mathcal{Z}_{D\bar{D}}[T] \equiv & \sum_{[K]} \prod_{i_L=1}^{K_L} \prod_{i_M=1}^{K_M} \prod_{i_{\bar{L}}=1}^{K_{\bar{L}}} \prod_{i_{\bar{M}}=1}^{K_{\bar{M}}} \int \frac{f d^3 x_{L i_L}}{K_L!} \frac{f d^3 x_{M i_M}}{K_M!} \\ & \times \frac{f d^3 y_{\bar{L} i_{\bar{L}}}}{K_{\bar{L}}!} \frac{f d^3 y_{\bar{M} i_{\bar{M}}}}{K_{\bar{M}}!} \det(G[x]) \det(G[y]) \\ & \times e^{-V_{D\bar{D}}(x-y)}, \end{aligned} \quad (10)$$

with $G[x]$ a $(K_L + K_M)^2$ matrix and $G[y]$ a $(K_{\bar{L}} + K_{\bar{M}})^2$ matrix whose explicit forms are given in [4,5].

B. Classical dyon-antidyon interactions

The explicit form of the Coulomb asymptotic in (10) for the SU(2) case is

$$\begin{aligned} V_{D\bar{D}}(x-y) \\ \rightarrow -\frac{C_D}{\alpha_s T} \left(\frac{1}{|x_M - y_{\bar{M}}|} + \frac{1}{|x_L - y_{\bar{L}}|} - \frac{1}{|x_M - y_{\bar{L}}|} - \frac{1}{|x_L - y_{\bar{M}}|} \right). \end{aligned} \quad (11)$$

The strength of the Coulomb interaction in (11) is C_D/α_s and is of order $1/\alpha_s$. It follows from the asymptotics of the streamline configuration. In Fig. 1 we show the attractive potential for the SU(2) streamline configuration in the $M\bar{M}$ channel [22]. The solid curve is a numerical fit to the data given by

$$V_{D\bar{D}}(r) \equiv s_{D\bar{D}} V(r) = s_{D\bar{D}} \frac{A v (r \cdot v - B)^2}{g^2 (r \cdot v)^3 + C}, \quad (12)$$

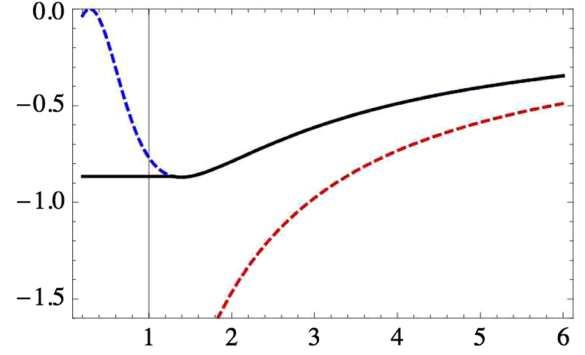


FIG. 1 (color online). Black solid line is the SU(2) $D\bar{D}$ (dimensionless) potential versus the distance r (in units of $1/T$). Upper (blue) dashed line is the parametrization proposed in Ref. [22], the lower (red) (dashed) line is the Coulomb asymptotics.

with $s_{M\bar{M}} = -1$ in units of the critical temperature T_c and g set to 1 and $A = 30.9$, $B = 0.9072$, $C = 15.795$. The dashed line corresponds to the Coulomb asymptotics,

$$V_{M\bar{M}}(r) \approx -\frac{C_D}{\alpha_s r}, \quad (13)$$

with $C_D = A/4\pi = 2.46$. We recall that in the uncombed $D\bar{D}$ potential, the asymptotic Coulomb interaction corresponds to $C_D = 2$. The attraction in the streamline is stronger asymptotically owing to the relative combing between the dyons. Figure 1 shows that the $D\bar{D}$ core is about $a_{D\bar{D}} \approx 1/T$. The second observation is that one should not use the Coulomb asymptotic (the lower dashed curve) but the actual potential which correctly takes care of the dyons as extended charged objects rather than point charges.

Below the core value of $a_{D\bar{D}}$, the streamline configuration annihilates into perturbative gluons making the parametrization (12) arbitrary. Throughout, we will parametrize the core by a constant, replacing (12) by

$$V_{D\bar{D}}(r) \equiv s_{D\bar{D}} (V(r)\theta(r - a_{D\bar{D}}) + V(a_{D\bar{D}})\theta(a_{D\bar{D}} - r)) \quad (14)$$

with $s_{M\bar{M}} = s_{L\bar{L}} = -1$ (attractive) and $s_{L\bar{M}} = s_{M\bar{L}} = +1$ (repulsive).

The ensemble (10) can be viewed as a 4-component dense and strongly coupled liquid. The quantity in the exponent, known as the classical plasma parameter,

$$\Gamma_{D\bar{D}} = V(a_{D\bar{D}}) \approx \frac{C_D/\alpha_s a_{D\bar{D}}}{3T_c} \approx 1, \quad (15)$$

is not small. Its exponent $e^{\Gamma_{D\bar{D}}}$ can even be large. This implies that the ‘‘dyonic plasma’’ we want to study belongs to a class of strongly coupled plasmas, with non-negligible

correlations between the particles. So *a priori*, this problem should be studied by methods more powerful than the usual mean field approximations, such as the Debye-Huckel theory. However, we will show below that when the dyonic densities are sufficiently large (and that implies the overall T of the ensemble to be sufficiently low), the screening mass gets large enough to put the effective—screened—interaction inside the domain in which the analytic Debye-Huckel theory becomes justified.

Furthermore, as we will detail below, the treatment of the repulsive core is in fact a rather sensitive issue. We chose the “most smooth” version of the potential, shown by the solid curve in Fig. 1. Its Fourier transform provides a smooth form factor in momentum space. We note that the actual streamline was only found for distances $r > a_{D\bar{D}} \approx 1.2$ (about $4/v$ in the dyon units). The upper (blue) dashed curve is an example of an arbitrary parametrization discussed in [22], extending it to smaller values of r . If one uses it, or even cut off the small $r < a_{D\bar{D}}$ region completely—the approach known as hard core or excluded volume—the Fourier transform of the potential develops large oscillations. In this case the instability of the Debye-Huckel theory becomes stronger and its applicability domain shrinks.

The use of (12) in the repulsive channels $M\bar{L}$ and $L\bar{M}$ approximates a smaller repulsion than Coulomb at shorter distances. A numerical investigation of these channels would be welcome. Note that both the measure in (10) and the asymptotic (11) do not include the quantum corrections around the streamline configuration. Both of which should add more repulsion to the interaction between D and \bar{D} . A leading quantum correction to the asymptotic (11) follows by analogy from the Coulomb corrections emerging from the DD and $\bar{D}\bar{D}$ determinantal interactions. In our case they are repulsive and amount to the shift

$$C_D \rightarrow C_D - \frac{2\alpha_s}{\pi} + \mathcal{O}(\alpha_s^2) \quad (16)$$

in the Coulomb constant. The relevance of this correction will be briefly discussed below.

C. Qualitative effect of the one-loop moduli space

The volume element of the moduli space of self-dual $SU(2)$ dyons is given by $\sqrt{g_{HK}} \equiv \det G$ with g_{HK} its associated Hyper-Kähler metric [4]. As we already mentioned in the Introduction, the one-loop determinant in the measure (2) must be positive definite for all configurations. Furthermore, the positivity of all eigenvalues is required, since they have the meaning of the volume element in the corresponding subspace. As noted in [21], this is not the case for ensembles with randomly placed dyons. These ensembles get denser, and the positivity condition is only fulfilled for a very small fraction of the configurations.

In fact, one of the main issues of the dyonic ensembles is the nontrivial character of the one-loop interaction induced by the Diakonov determinant. Before we show how this carries to our case through various fermionization and bosonization and diagrammatic re-summations, it is instructive to provide a qualitative understanding of the issues using simple explicit examples.

Although it is well known, for completeness let us start with the simplest case of two dyons in the $SU(2)$ theory with symmetric holonomy $\nu = \bar{\nu} = 1/2$. Omitting the overall factors, Diakonov 2×2 matrix G reads

$$G_{2 \times 2}[x] \sim \begin{pmatrix} 1 \pm \frac{1}{vx_{12}} & \mp \frac{1}{vx_{12}} \\ \mp \frac{1}{vx_{12}} & 1 \pm \frac{1}{vx_{12}} \end{pmatrix} \quad (17)$$

with $x_{12} \equiv |\vec{x}_{(1)} - \vec{x}_{(2)}|$ the distance between the dyons in units of $1/v = 1/\pi T$. The upper signs are for different (ML) dyons, and the lower for similar (MM, LL) pairs. The metric-induced potential is, thus, $V(x_{12}) \equiv -\ln \det G = -\ln(1 \pm 2/(vx_{12})) \approx \mp 2/(vx_{12})$ is Coulomb-like at large distances. (At short distances the induced potential is proportional to $\ln(1/r)$ and not $1/r$. There is no divergence in the partition function.)

Let us now consider an ensemble of several ($N = 8$) dyons with $N_M = N_L = 4$ and set them randomly in a cube of size a . We then evaluate all interdyon distances and calculate $\det G[x]$ (which is now an 8×8 matrix) as a function of the Coulomb parameter $\epsilon = 1/(\pi a T)$. For each sampling, the determinant is a polynomial of ϵ of degree N . The results of ten random samplings are displayed in Fig. 2 by the dashed lines. For small ϵ the determinant deviates from 1 in a nonuniform way. Some configurations are Coulomb attractive with $\det G > 1$, while some others are

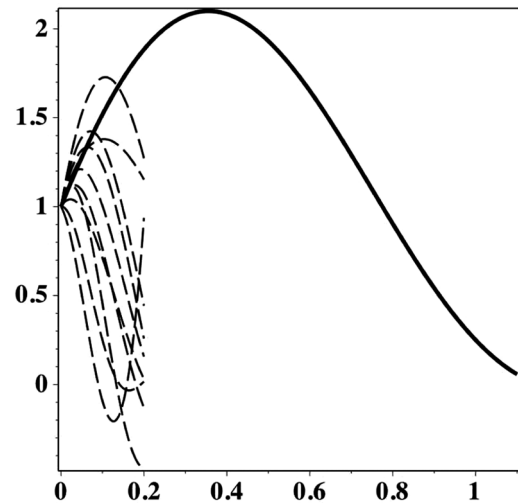


FIG. 2. $\det G$ as a function of $\epsilon = 1/(\pi a T)$. The dashed lines are for eight dyons randomly placed in a cube of size $a \equiv 1$. The solid line is for correlated dyons in a saltlike or fcc configuration also in a unit cube.

repulsive with $\det G < 1$ for small ϵ . To first order, they average to zero for a large number of charges as there are equal number of positive and negative ones. At next order, the attraction is to win, thanks to the general theorem of second-order perturbation theory. However, we observe that already for $\epsilon = 1/(\pi a T) \sim 0.2$ the repulsive trend is dominant and $\det G < 0$ for some samplings. This means that the moduli space of these configurations vanishes at the corresponding density. This sets an upper limit on the density of random ensembles of dyons,

$$n < n_{\max} = 8(0.2\pi T)^3 \sim 1.98T^3. \quad (18)$$

The lesson: Diakonov determinantal interaction for randomly placed dyons is strongly repulsive, reducing dramatically the moduli space all the way to zero size for small ϵ . It amounts to a strong effective core of order α_s^0 .

However, this is not the end of the story. Let us look at the opposite case of a well-ordered arrangement of dyons in the unit box. For that and for illustrative purposes only, we prearrange the eight dyons of the previous ensemble in a saltlike or fcc configuration on the unit cube, and assess the corresponding $\det G$. The result is shown in Fig. 2 by the solid line. While the qualitative trend is the same—attraction at some interval of densities, changing to repulsion and then reaching zero at some density—the value of the maximal density to be reached is changed by a large factor of about $5^3 = 125$. Here is lesson number two: the moduli space can be made much larger for the same interparticle Coulomb strength ϵ if the correlations between charges are correctly taken into account.

The overall lesson we get from those examples is the following: Diakonov's original suggestion that attraction and repulsion would always cancel can be overcome. Our analysis shows that ultimately the repulsion wins at some density where the volume of the moduli space goes to zero. However, correctly implemented correlations between charges to maximize screening locally can increase this critical density by about 2 orders of magnitude. Clearly, the present setup acts as a good toy model for confinement in the parameter range stated.

D. Fermionization and bosonization

Following [4] each determinant in (10) can be fermionized using four pairs of ghost fields $\chi_{L,M}^\dagger, \chi_{L,M}$ for the dyons and four pairs of ghost fields $\chi_{\bar{L},\bar{M}}^\dagger, \chi_{\bar{L},\bar{M}}$ for the antidions. The ensuing Coulomb factors from the determinants are then bosonized using four boson fields $v_{L,M}, w_{L,M}$ for the dyons and similarly for the antidions. The result is a doubling of the three-dimensional free actions obtained in [4]

$$\begin{aligned} S_{1F}[\chi, v, w] &= -\frac{T}{4\pi} \int d^3x (|\nabla\chi_L|^2 + |\nabla\chi_M|^2 + \nabla v_L \cdot \nabla w_L + \nabla v_M \cdot \nabla w_M) \\ &\quad + (|\nabla\chi_{\bar{L}}|^2 + |\nabla\chi_{\bar{M}}|^2 + \nabla v_{\bar{L}} \cdot \nabla w_{\bar{L}} + \nabla v_{\bar{M}} \cdot \nabla w_{\bar{M}}). \end{aligned} \quad (19)$$

For the interaction part $V_{D\bar{D}}$, we note that the pair Coulomb interaction in (11) between the dyons and antidions can also be bosonized using the standard trick [12] in terms of σ and b fields. Here σ and b are the un-Higgsed long range U(1) parts of the original magnetic field F_{ij} and electric potential A_4 (modulo the holonomy), respectively. As a result, each dyon species acquire additional fugacity factors such that

$$M: e^{-b-i\sigma} \quad L: e^{b+i\sigma} \quad \bar{M}: e^{-b+i\sigma} \quad \bar{L}: e^{b-i\sigma}. \quad (20)$$

These assignments are consistent with those suggested in [16,18] using different arguments. As a result there is an additional contribution to the free part (19)

$$\begin{aligned} S_{2F}[\sigma, b] &= T \int d^3x d^3y (b(x)V^{-1}(x-y)b(y) + \sigma(x)V^{-1}(x-y)\sigma(y)) \end{aligned} \quad (21)$$

with $V(r)$ defined in (12). The interaction part is now

$$\begin{aligned} S_I[v, w, b, \sigma, \chi] &= - \int d^3x e^{-b+i\sigma} f(4\pi v_m + |\chi_M - \chi_L|^2 + v_M - v_L) e^{w_M - w_L} \\ &\quad + e^{b-i\sigma} f(4\pi v_l + |\chi_L - \chi_M|^2 + v_L - v_M) e^{w_L - w_M} \\ &\quad + e^{-b-i\sigma} f(4\pi v_{\bar{m}} + |\chi_{\bar{M}} - \chi_{\bar{L}}|^2 + v_{\bar{M}} - v_{\bar{L}}) e^{w_{\bar{M}} - w_{\bar{L}}} \\ &\quad + e^{b+i\sigma} f(4\pi v_{\bar{l}} + |\chi_{\bar{L}} - \chi_{\bar{M}}|^2 + v_{\bar{L}} - v_{\bar{M}}) e^{w_{\bar{L}} - w_{\bar{M}}}. \end{aligned} \quad (22)$$

In terms of (19)–(22) the dyon-antidyon partition function (9) can be exactly re-written as an interacting effective field theory in three dimensions,

$$\mathcal{Z}_{D\bar{D}}[T] \equiv \int D[\chi] D[v] D[w] D[\sigma] D[b] e^{-S_{1F} - S_{2F} - S_I}. \quad (23)$$

In the absence of the screening fields σ, b (23) reduces to the three-dimensional effective field theory discussed in [4] which was found to be integrable. In the presence of σ, b the integrability is lost as the dyon-antidyon screening upsets the hyper-Kähler nature of the moduli space. We will investigate them by linearizing the screening effects in the symmetric state.

Since the effective action in (23) is linear in the $v_{M,L,\bar{M},\bar{L}}$, the latter are auxiliary fields that integrate into delta-function constraints. However and for convenience, it is best to shift away the b, σ fields from (22) through

$$\begin{aligned} w_M - b + i\sigma &\rightarrow w_M \\ w_{\bar{M}} - b - i\sigma &\rightarrow w_{\bar{M}}, \end{aligned} \quad (24)$$

which carries unit Jacobian and no anomalies, and recover them in the pertinent arguments of the delta function constraints as

$$\begin{aligned} -\frac{T}{4\pi}\nabla^2 w_M + f e^{w_M - w_L} - f e^{w_L - w_M} &= \frac{T}{4\pi}\nabla^2(b - i\sigma) \\ -\frac{T}{4\pi}\nabla^2 w_L + f e^{w_L - w_M} - f e^{w_M - w_L} &= 0 \end{aligned} \quad (25)$$

and similarly for the antidyons. In [4] it was observed that the classical solutions to (25) can be used to integrate the w 's in (23) to one loop. The resulting bosonic determinant was shown to cancel against the fermionic determinant after also integrating over the χ 's in (23). This holds for our case as well. However, the presence of σ, b makes the additional parts of (23) still very involved in three dimensions.

After inserting the constraints in the three-dimensional effective action in (23), the ground state corresponds to constant fields because of translational invariance. Thus, the potential per unit 3-volume V_3 following from (22) after the shifts (24) is

$$\begin{aligned} -\mathcal{V}/V_3 &= 4\pi f(v_m e^{w_M - w_L} + v_l e^{w_L - w_M}) \\ &+ 4\pi f(v_{\bar{m}} e^{w_{\bar{M}} - w_L} + v_{\bar{l}} e^{w_L - w_{\bar{M}}}). \end{aligned} \quad (26)$$

Note that if we did not perform the shift (24) then both the potential (26) and the constraints (25) depend on b and σ making the extrema search for \mathcal{V} more involved. Of course the results should be the same. For fixed holonomies $v_{m,l}$, the constant w 's are real by (25) as all right hand sides vanish, and the extrema of (26) occur for

$$\begin{aligned} e^{w_M - w_L} &= \pm \sqrt{v_l/v_m} \\ e^{w_{\bar{M}} - w_L} &= \pm \sqrt{v_{\bar{l}}/v_{\bar{m}}} \end{aligned} \quad (27)$$

(27) is only consistent with (25) if and only if $v_l = v_m = 1/2$ and $v_{\bar{l}} = v_{\bar{m}} = -1/2$. That is for confining holonomies or a center symmetric ground state. However and because of the constraint (25) there is no effective potential for the holonomies in the interacting dyon-antidyon liquid. Indeed, by enforcing (25) before variation we have $\mathcal{V}/V_3 = -n_D$, whatever the v 's. On this point we differ from the arguments and corresponding results made in [4] where the constraints (25) were not enforced before the variational derivation of the holonomy potential. Note that the alternative argument in [4] in favor of the holonomy potential fixes the number of dyon species K_i to be equal *a priori*, while (10) fixes it only on the average.

III. LINEARIZED SCREENING APPROXIMATION IN CENTER SYMMETRIC STATE

For the center symmetric ground state of the three-dimensional effective theory, we may assess the correction to the potential \mathcal{V} to one-loop in the b, σ fields. This is achieved by linearizing the constraints (25) around the ground state solutions. Specifically

$$\begin{aligned} \left(-\frac{T}{4\pi}\nabla^2 + 2f\right)w_M - 2fw_L &\approx \frac{T}{4\pi}\nabla^2(b - i\sigma) \\ \left(-\frac{T}{4\pi}\nabla^2 + 2f\right)w_L - 2fw_M &\approx 0 \end{aligned} \quad (28)$$

and similarly for the antidyons. The one-loop correction to \mathcal{V} follows by inserting (28) in (23). The ensuing quadratic contributions before integrations are

$$S_{1L} = \mathcal{V} - 4\pi f \int \frac{d^3 p}{(2\pi)^3} \frac{\left(\frac{T}{4\pi} p^2\right)^2}{\left(\frac{T}{4\pi} p^2 + 4f\right)^2} (b(p)^2 - \sigma(p)^2). \quad (29)$$

The coefficient of the b field appears tachyonic but is momentum dependent and vanishes at zero momentum.

A. Pressure

Carrying the Gaussian integration in b, σ in (29) yields to one-loop

$$\ln Z_{1L}/V_3 = -\mathcal{V} - \frac{1}{2} \int \frac{d^3 p}{(2\pi)^3} \ln \left| 1 - \frac{V^2(p)}{16} \frac{p^8 M^4}{(p^2 + M^2)^4} \right| \quad (30)$$

with $V(p)$ the Fourier transform of (12)

$$V(p) = \frac{4\pi}{p^2} \int_0^\infty dr \sin r V_{D\bar{D}}(r/p) \quad (31)$$

and the screening mass $M = \sqrt{2n_D/T}$ with $|Q^2| = 2$ for SU(2). In Fig. 3 we show the form factor (31) in dots line in units of T_c . A simple parametrization is shown in solid line of the form

$$V(p) \approx 4\alpha \frac{e^{-p a_{D\bar{D}}}}{p^2} \cos(p a_{D\bar{D}}) \quad (32)$$

with $\alpha = \pi C_D/\alpha_s$ and a core $a_{D\bar{D}} \approx 1/T_c$. Inserting (32) into (30) and setting $\tilde{p} = p/M$ yield

$$\ln Z_{1L}/V_3 = -\mathcal{V} - \frac{M^3}{2} \int \frac{d^3 \tilde{p}}{(2\pi)^3} \ln \left| 1 - \tilde{\alpha}^2(\tilde{p}) \frac{\tilde{p}^4}{(\tilde{p}^2 + 1)^4} \right| \quad (33)$$

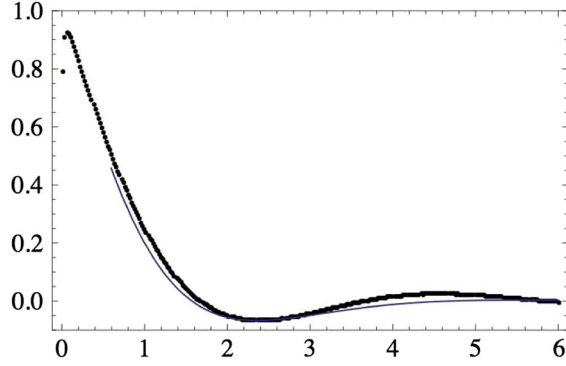


FIG. 3 (color online). The dots show the form factor, the ratio $V(p) \cdot (p^2/4\pi)$ of the Fourier transform of (12) to that of a pure Coulomb law versus p/T . The thin line is its parametrization. See text.

with

$$\tilde{\alpha}(\tilde{p}) \equiv \alpha e^{-Ma_{D\tilde{D}}\tilde{p}} \cos(Ma_{D\tilde{D}}\tilde{p}). \quad (34)$$

The dominant contribution to the integral in (30) comes from the region $\tilde{p} \approx 1$ for which (34) can be approximated by $\tilde{\alpha}(1) \equiv \tilde{\alpha}$. As a result (30) can be done approximately by fixing $\tilde{\alpha}$ and we have the classical contribution to the pressure

$$\frac{\mathcal{P}_{\text{cl}}}{T} \equiv \ln Z_{1L}/V_3 \approx n_D + \kappa(\tilde{\alpha}) \frac{M^3}{12\pi} \quad (35)$$

with

$$\kappa(\tilde{\alpha}) = \frac{2 + \frac{5}{2}\tilde{\alpha} + \frac{1}{2}\tilde{\alpha}^2}{\sqrt{1 + \frac{\tilde{\alpha}}{4}}} + \frac{2 - \frac{5}{2}\tilde{\alpha} + \frac{1}{2}\tilde{\alpha}^2}{\sqrt{1 - \frac{\tilde{\alpha}}{4}}} - 4 \quad (36)$$

(36) is seen to vanish for $\tilde{\alpha} = 0$ or in the absence of $D\tilde{D}$ interactions. Near T_c the screening mass is $M \approx \sigma_E/T_c$ (see below), thus

$$\tilde{\alpha} \equiv (\pi C_D/\alpha_s) e^{-Ma_{D\tilde{D}}} \cos(Ma_{D\tilde{D}}) \approx -0.52. \quad (37)$$

For $|\tilde{\alpha}| < 4$ the 1-loop contribution to the pressure from the charged $D\tilde{D}$ dyons is real with no dimer or molecular instability. The large core produced by the form factor (34) is considerably screened by the large dyon density as captured by the large dielectric constant $1/\kappa(-0.52) \approx 5.26$ in (35).

The correction in (35) to the free contribution is a Debye-Huckel correction [23] (and references therein). A simple but physical way to understand it is to note that a screened Coulomb charge carries a lower constant energy

$$\frac{e^{-M|x|}}{4\pi|x|} \approx \frac{1}{4\pi|x|} - \frac{M}{4\pi} + \dots \quad (38)$$

The Debye-Huckel as a mean-field estimate for the pressure follows

$$\frac{\mathcal{P}_{\text{DH}}}{T} \approx \frac{n_D M}{4\pi T} = \frac{M^3}{8\pi} \rightarrow \frac{M^3}{12\pi}, \quad (39)$$

where $n_D = M^2 T/2$ is the density of charged particles (see below). The standard Debye-Huckel limiting result for a multi-component ionic plasma in three spatial dimensions is shown on the right-most side of (39).

The correction in (35) is considerably reduced by the large screening through the effective dielectric constant played by $1/\kappa(\tilde{\alpha}) \approx 32/(15\tilde{\alpha}^2)$ for $\tilde{\alpha} \ll 1$. In particular $1/\kappa(-0.52) \approx 5.26 \gg 1$ as noted earlier. It can be recast in the form

$$\frac{\mathcal{P}_{\text{cl}}}{T^4} = \tilde{n}_D + \frac{\kappa(\tilde{\alpha})}{3\pi\sqrt{2}} \tilde{n}_D^{\frac{3}{2}} \quad (40)$$

with $\tilde{n}_D = n_D/T^3$. Using $Ma_{D\tilde{D}} \approx \sigma_E/T_c^2 \approx 1/(0.71)^2$ for SU(2) we have $\tilde{n}_D \approx 1$, so that $\mathcal{P}_{\text{cl}}/T^4 \approx (1 + 0.01)$. The screening corrections are small of the order of 1% thanks to the large dyonic densities.

The limitations of the Debye-Huckel approximation are readily seen from (30). In Fig. 4a we plot the argument of the logarithm in the last term of (30). The different curves from top to bottom follow from $Ma_{D\tilde{D}} = 1.5, 1, 0.7, 0.56$, respectively. The smaller the Debye mass M the stronger the dip. For $Ma_{D\tilde{D}} < 0.56$, the argument of the logarithm becomes negative resulting into an $i\pi$ contribution to the pressure and thus an instability. This is a clear indication of a well-known phenomenon: the Debye-Huckel approximation is, in general, inapplicable for strongly coupled plasmas, and the interaction mediated by the streamline is strong. Only a large enough density of dyons, producing sufficiently strong screening, allows for the use of the Debye-Huckel theory. In Fig. 4(b) we show how the total integrated contribution to the free energy changes as a function of the dimensionless Debye mass $Ma_{D\tilde{D}}$:

$$(Ma_{D\tilde{D}})^3 \int_0^\infty dp p^2 \ln \left| 1 - \frac{V^2(pM)}{16} \frac{p^8}{(p^2 + 1)^4} \right|. \quad (41)$$

The main lesson is that beyond the critical value of the screening, this contribution rapidly becomes very small. This is consistent with the analytical estimate above. This justifies the use of the Debye-Huckel mean-field analysis, in general, and the use of the semiclassical expansion in particular.

B. Beyond the Debye-Huckel theory

The unraveling of the Debye-Huckel approximation may be due to corrections to an interacting Coulomb system, such as (i) core corrections and (ii) dimer, tetramer, and so on many-body interactions. The large core corrections were

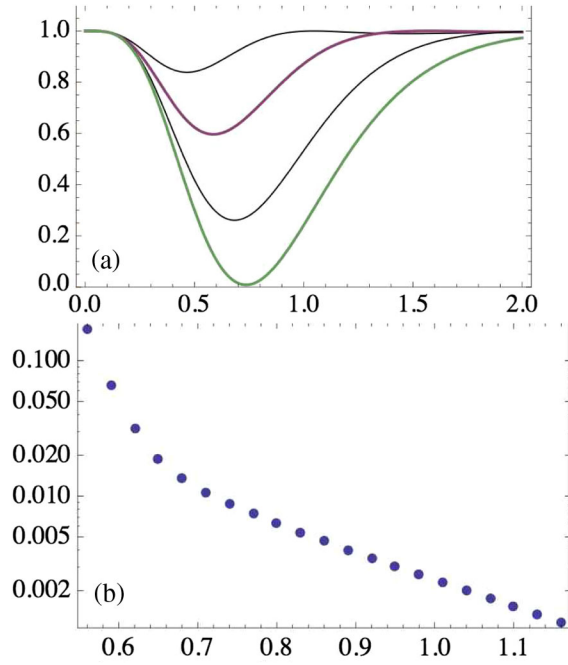


FIG. 4 (color online). (a) The argument of the logarithm in the last term of (30) versus the dimensionless momentum p , for different values of the dimensionless Debye mass $Ma_{D\bar{D}} = 1.5, 1, 0.7, 0.56$, top to bottom. As the screening mass decreases to its critical value, the lower (green) curve touches zero. The smaller values of M lead to a negative argument of the logarithm, thus an instability. (b) A semilogarithmic plot of the integral entering in (30) as defined in (41) as a function of $Ma_{D\bar{D}}$. The decrease is steady from its maximum at the critical value of the screening mass or $Ma_{D\bar{D}} = 0.56$.

already identified and discussed above and yield a substantial reduction in the Debye-Huckel contribution near the critical value of $Ma_{D\bar{D}} \sim 0.56$.

Bound state corrections in the form of electrically charged $L\bar{L}$ or $M\bar{M}$ dimers, or electrically neutral $L\bar{L}M\bar{M}$ tetramers commonly referred to as instanton-anti-instanton molecules, can bind through the streamline interaction (11) and (12). The combinations $L\bar{M}$ and $M\bar{L}$ are repulsive. The binding energy in a dimer is $\epsilon_{D\bar{D}} \approx (C_D/3)/(\alpha_s a_{D\bar{D}}) = T$. The dimer enhancement is expected to be of order $e^{\epsilon_{D\bar{D}}/T} \approx e^{(C_D/3)/\alpha_s} \approx 2.72$ for $T \approx T_c$ using the reduced effective Coulomb coupling. As we noted earlier, this enhancement becomes substantially larger at high temperature as α_s decreases with the onset of dimerization set at about $\alpha_{s,\text{crit}} = \pi(C_D/3)/4 \approx 0.67$. At this coupling which occurs above T_c , the Coulomb dimer enhancement factor is $e^{C_D/3\alpha_{s,\text{crit}}} \approx 3.57$.

In sum, the dyons and antidyons form a Coulomb liquid with strong short-range correlations induced by both the finite cores and bindings. The liquid supports center symmetry and confines. The deconfinement transition is characterized by clustering into charged dimers and possibly uncharged and topologically neutral tetramers,

forming mixtures with the restoration of center symmetry. Coulomb mixtures present rich phase diagrams [26].

C. Dyonic densities

Equation (30) can be readily used to assess the dyon densities K_M and K_L (and similarly for $K_{\bar{M}}$ and $K_{\bar{L}}$) in the center symmetric vacuum with screening dyons-antidyons. For that we need to change $f \rightarrow \sqrt{f_M f_L}$ and take derivatives of (30) with respect to $\ln f_{M,L}$ separately and then set them equal by bulk charge neutrality. The result per species is

$$K = \frac{1}{4}n_D + \kappa(\tilde{\alpha})\frac{M^3}{32\pi} \quad (42)$$

for all dyon and antidyon species.

Each dyon (antidyon) is characterized by an $SU(2)$ core of size $\rho \approx 1/(2\pi T\nu) \approx 0.33$ fm in the center symmetric phase with $\nu = 1/2$ at $T = 1/\text{fm}$. The Debye length $\lambda_D = 1/M \approx \sqrt{T/2n_D} \approx 0.70$ fm is about twice the core size. The classical Coulomb ratio for the $DD, \bar{D}\bar{D}$ pairs with a core of 2ρ is about

$$\Gamma_{DD,\bar{D}\bar{D}} \equiv \frac{1}{2\pi(2\rho)T} \approx \frac{\nu}{2} = \frac{1}{4}, \quad (43)$$

which is small. Recall from (15) that $\Gamma_{D\bar{D}} \approx 1$. The Coulomb $DD, \bar{D}\bar{D}$ interactions are quantum and of order α_s^0 with strength $1/\pi$ as can be seen by expanding the exponential form of the determinantal interaction in (17). The dyon-antidyon ensemble is close to a strongly coupled 4-component Coulomb liquid. Since the measure for the unlike dyons is exact, it is valid even in the dense configuration. It is only asymptotically exact for like dyons. For the dyons and antidyons, the streamline is numerically exact at all separations outside its core. However, its corresponding quantum determinant was not calculated. Only a qualitative correction was argued in (24).

D. Gluon condensates and susceptibilities

The topological charge fluctuates locally in this dyon-antidyon model. The topological susceptibility at one loop follows from (30) through the substitution $f \rightarrow f \cos(\theta/2)$ both in \mathcal{V} and also $M \rightarrow M\sqrt{\cos(\theta/2)}$. At finite vacuum angle θ and in leading order, we have

$$\begin{aligned} \langle F\tilde{F} \rangle_\theta &\equiv -\frac{T}{V_3} \frac{\partial \ln Z_{1L}}{\partial \theta} \\ &= \sin(\theta/2) \left(\frac{1}{2}n_D T + \kappa(\tilde{\alpha}) \frac{M^3 T}{16\pi} \sqrt{\cos(\theta/2)} \right). \end{aligned} \quad (44)$$

Thus, we have the topological susceptibility

$$\chi_T \equiv \frac{V_3}{T} \langle (F\tilde{F})^2 \rangle_0 \approx \left(\frac{1}{2}\right)^2 (n_D T) \quad (45)$$

in leading order. Since the dyons carry half the topological charge, Eq. (45) shows that the topological fluctuations are Poissonian to order $\mathcal{O}(n_D^{3/2})$. The behavior of χ_T/T^4 versus T/T_c is shown in Fig. 5 with n_D defined in (56) below.

The gluon condensate to one loop in the screening approximation follows from

$$\begin{aligned} \frac{1}{16\pi^2} \langle F^2 \rangle_0 &\equiv -\frac{T}{4\pi V_3} \frac{\partial \ln Z_{1L}}{\partial 1/\alpha_s} \\ &\approx -\frac{T}{4\pi} \left(\frac{2}{\alpha_s} - \pi\right) \left(n_D + \frac{\kappa(\tilde{\alpha})M^3}{8\pi}\right), \end{aligned} \quad (46)$$

which is non-Poissonian because of the scale anomaly. The compressibility of the ground state is

$$\begin{aligned} \sigma_\chi &\equiv \frac{V_3}{T} \left\langle \left(\frac{F^2}{16\pi^2}\right)^2 \right\rangle_c \\ &\approx \frac{T}{16\pi^2} \left(2\left(n_D + \frac{\kappa M^3}{8\pi}\right) + \left(\frac{2}{\alpha_s} - \pi\right)^2 \left(n_D + \frac{3\kappa M^3}{16\pi}\right)\right) \end{aligned} \quad (47)$$

for the connected correlator.

We can use (35) and (46) to extract the electric $\langle E^2 \rangle_0$ and magnetic $\langle B^2 \rangle_0$ condensates in the dyonic ensemble. For that we note that the energy per volume in Euclidean space follows from (35) through

$$\frac{1}{8\pi} \langle B^2 - E^2 \rangle_0 = T^2 \frac{\partial P_{\text{cl}}}{\partial T} \frac{1}{T}. \quad (48)$$

The results are

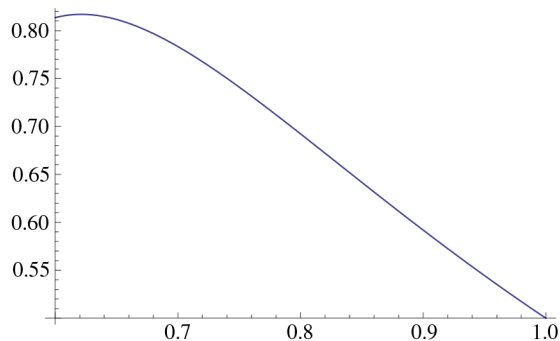


FIG. 5 (color online). Topological susceptibility in units of T versus T/T_c .

$$\begin{aligned} \frac{\langle B^2 \rangle_0}{4\pi T} &= \left(+3 - \left(1 + \frac{2\alpha'_s}{\alpha_s^2}\right) \left(\frac{1}{\alpha_s} - \frac{\pi}{2}\right)\right) \left(n_D + \frac{\kappa M^3}{8\pi}\right) \\ \frac{\langle E^2 \rangle_0}{4\pi T} &= \left(-3 - \left(1 - \frac{2\alpha'_s}{\alpha_s^2}\right) \left(\frac{1}{\alpha_s} - \frac{\pi}{2}\right)\right) \left(n_D + \frac{\kappa M^3}{8\pi}\right), \end{aligned} \quad (49)$$

with $\alpha'_s = \partial\alpha_s/\partial \ln T$. In Fig. 6 we show the behavior of the chromoelectric condensate $\langle E^2 \rangle$ (solid-black), the chromomagnetic condensate $\langle B^2 \rangle$ (dashed-blue), and the (Euclidean) energy density $\langle B^2 - E^2 \rangle$ (dot-dashed-brown) in units of T versus T/T_c in the center symmetric phase. We used the dyon density fixed in (56) below. The chromomagnetic condensate is about constant in the range of $0.6 < T/T_c < 1$ while the chromoelectric condensate decreases monotonously. The condensates are about equal and opposite near T_c , a point supported by the lattice extracted condensates in [25]. We note that the lattice analysis in [25] involves a specific subtraction of the black-body contribution which we do not have in our semi-classical analysis.

E. Electric and magnetic screening masses

The center symmetric phase of the dyon-antidyon liquid screens the long-range U(1) gauge fields left un-Higgsed by the holonomy $A_4(\infty)/2\pi T = \nu T^3/2$. The electric and magnetic correlations in these Abelian U(1) charges can be obtained by introducing the U(1) Abelian sources $\eta_{m,e}$ for the magnetic and electric charge densities,

$$\rho_{m,e}(x) = \sum_i Q_{m,e,i} \delta^3(x - x_i), \quad (50)$$

with $|Q_{m,e}| = 1$, and shifting the U(1) fields $\sigma \rightarrow \sigma + \eta_m$ and $b \rightarrow b + \eta_e$ in the three-dimensional effective action. To one loop, the generating functional for the charge density correlators is

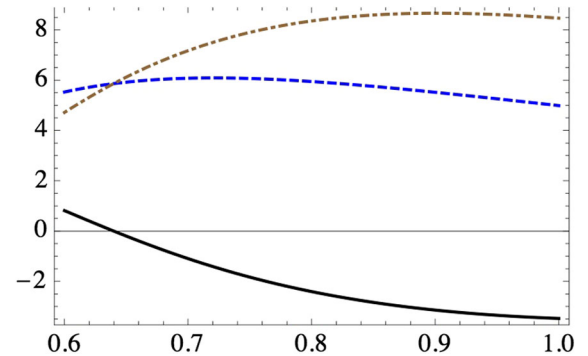


FIG. 6 (color online). The electric $\langle E^2 \rangle$ (solid-black), magnetic $\langle B^2 \rangle$ (dashed-blue), and (Euclidean) energy density $\langle B^2 - E^2 \rangle$ (dot-dashed-brown) in units of T versus T/T_c . See text.

$$Z_{1L}[\eta_m, \eta_e] = \int D[\sigma] D[b] e^{-S_{2F}[\sigma, b] - S_{1L}[\sigma + \eta_m, b + \eta_e]}, \quad (51)$$

which is Gaussian in the sources and, therefore, readily integrated out. Thus,

$$\ln Z_{1L}[\eta_m, \eta_e] = - \int \frac{d^3 p}{(2\pi)^3} \sum_{i=e,m} \eta_i(p) \mathbf{G}_i(p) \eta_i(-p), \quad (52)$$

with the electric and magnetic density correlators following by variation,

$$\begin{aligned} \mathbf{G}_{m,e}(p) &\equiv \frac{1}{V_3} \langle |\rho_{m,e}(p)|^2 \rangle \\ &\approx \frac{1}{4} \frac{TM^2 p^4}{(p^2 + M^2)^2 \pm \tilde{\alpha} M^2 p^2}, \end{aligned} \quad (53)$$

with the upper sign for magnetic and the lower sign for electric. In x space, (53) can be inverted by Fourier transforms. The result for the electric correlator in spatial coordinates is

$$\begin{aligned} &-\frac{TM^4}{16\pi|x|} e^{-\sqrt{1-\frac{\tilde{\alpha}}{4}}M|x|} \\ &\times \left[\cos\left(\frac{\sqrt{\tilde{\alpha}}}{2}M|x|\right) (\tilde{\alpha}-2) + \sin\left(\frac{\sqrt{\tilde{\alpha}}}{2}M|x|\right) \frac{1-2\tilde{\alpha}+\frac{\tilde{\alpha}^2}{2}}{\sqrt{\tilde{\alpha}(1-\frac{\tilde{\alpha}}{4})}} \right]. \end{aligned} \quad (54)$$

The magnetic correlator follows by analytical continuation through the substitution $\tilde{\alpha} \rightarrow -\tilde{\alpha}$ in (54). The electric screening masses $M_{M,E}$ follow from the large-distance asymptotics. Using our estimate of $\tilde{\alpha} \approx -0.52 < 0$ from the Debye-Huckel analysis above, we have

$$\begin{aligned} \frac{M_E}{M} &\approx \left(\sqrt{1 + \frac{|\tilde{\alpha}|}{4}} - \frac{\sqrt{|\tilde{\alpha}|}}{2} \right) \approx 0.70 \\ \frac{M_M}{M} &\approx \left(\sqrt{1 - \frac{|\tilde{\alpha}|}{4}} \right) \approx 0.93, \end{aligned} \quad (55)$$

with $M^2 = 2n_D/T$. Also the arguments below show that $M = \sigma_E/T$. Combining these two results allows us to fix C in (5) above. Indeed, at T_c the SU(2) lattice results give $T_c/\sqrt{\sigma_E} \approx 0.71$. So Eq. (5) now reads

$$\frac{n_D}{T^3} \approx 2 \frac{\alpha_s^2(T_c)}{\alpha_s^2(T)} e^{\frac{\pi}{\alpha_s(T_c)} - \frac{\pi}{\alpha_s(T)}}, \quad (56)$$

which gives $M_E \approx 1.4$ and $M_M \approx 1.8T_c$, both of which are remarkably close to the reported SU(2) lattice results in the vicinity of the critical temperature [27]. In Fig. 7 we display the results (55) for $M_{E,M}/T$ in the range $(0.5-1)T_c$ versus

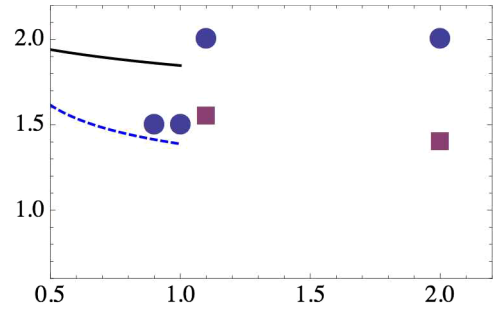


FIG. 7 (color online). The electric M_E/T (dashed line) and magnetic M_M/T (solid line) screening masses in (55) versus T/T_c . The points are SU(2) lattice data from [27] shown for comparison, (blue) circles are M_E/T , (red) squares are M_M/T .

T/T_c . The points at $T > T_c$ are shown for comparison. We note that the electric mass drops down at T_c . In the region we study $M_M > M_E$, while above T_c , in a more familiar QGP region, $M_M < M_E$. This switching of the magnitude of the two screening masses is better documented in lattice works with the $SU(3)$ gauge group. It has a simple explanation in our case. Since at $T > T_c$ the dyon density drops, it follows that M decreases as well. As a result, the form factor in Fig. 3 is probed at smaller momentum $p \approx M$ (larger distances) making $\tilde{\alpha}(p \approx M)$ in (34) switch from negative ($T < T_c$) to positive ($T > T_c$). From (53) it follows that the expressions for $M_{E,M}$ in (55) are now switched with M_M lighter than M_E . A simple estimate of the critical temperature at the crossing follows from the vanishing of (37) or $Ma_{D\bar{D}} = \pi/2$. This translates to a critical dyon density $n_D^C \approx \pi^2 T_c^3/8$ which is consistent with our estimate of T_c below (see (71)).

Finally, we note that the value of $\alpha_s(T_c) \approx 0.84$ extracted from the cooled caloron data in [19] is also consistent with the reported value from bulk thermodynamics in [28]. In the dyon-antidyon Coulomb liquid the correlators are modified at intermediate distances as we now detail in terms of the static structure factors.

F. Static structure factors

The charged structure factor between a pair of magnetic or electric charges is (53) which can be rewritten as

$$\mathbf{G}_{M,E}(p) \equiv \left\langle \frac{1}{N_{m,e}} \left| \sum_{j=1}^{N_{m,e}} Q_{m,e,j} e^{ik \cdot x_j} \right|^2 \right\rangle. \quad (57)$$

Thus,

$$\mathbf{G}_{M,E}(p) = \frac{\mathbf{G}_{m,e}(p)}{n_D/2} \equiv \frac{\tilde{p}^4}{(\tilde{p}^2 + 1)^2 \pm \tilde{\alpha} \tilde{p}^2}, \quad (58)$$

with $\tilde{p} = p/M$. We note that the prefactor in (58) involves two static electric or magnetic exchanges with an identical screening mass M . The charged structure factors vanish as

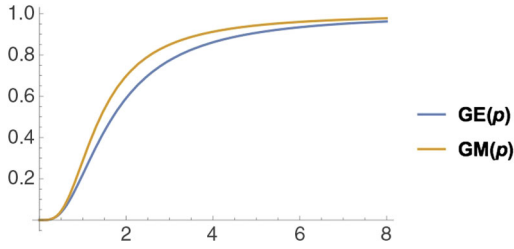


FIG. 8 (color online). The electric and magnetic structure factors (53) as a function of p/M .

$\mathbf{G}_{M,E}(p) \approx \tilde{p}^4$. For large momenta or $\tilde{p} \gg 1$ both structure factors asymptote one from below as shown in Fig. 8. The magnetic hole is slightly smaller than the electric one around the same pairs. The absence of oscillations in the structure factor is a consequence of our linearized approximation.

To characterize further the 4-component plasma of dyons and antidions, we define the scalar static pair correlation function,

$$\mathbf{G}_S(x) = \left\langle \frac{1}{N} \sum_{i \neq j}^N \delta^3(x + x_i - x_j) \right\rangle, \quad (59)$$

normalized to the total number of particles N . Equation (59) defines the probability to find two particles a distance $|x|$ apart. Its Fourier transform,

$$\mathbf{G}_S(p) = \left\langle \frac{1}{N} \left| \sum_{j=1}^N e^{ip \cdot x_j} \right|^2 \right\rangle, \quad (60)$$

is the scalar structure factor.

Equation (60) can be evaluated by switching $f \rightarrow f + \delta f(x_i)$ in (10) and then linearizing the resulting effective action around the mean density. Specifically, we can rewrite the linearized constraint (28) formally as

$$(w_M - w_L) = \frac{1}{\Delta_0 + 4\delta f} \left(\frac{T\nabla^2}{4\pi} \right) (b - i\sigma), \quad (61)$$

with $\Delta_0 = -T\nabla^2/4\pi + 4f$ and use perturbation theory to expand the denominator in (61) to order $\mathcal{O}(\delta f^3)$. The result can be formally written as

$$(w_M - w_L)(p) = \int \frac{d^3k}{(2\pi)^3} G(p, k) (b - i\sigma)(k). \quad (62)$$

Inserting (62) into the potential (26) yields a quadratic action in b and σ . Integrating over the latter yields the one-loop determinant or the effective action for $\delta \equiv \delta f/f$. Specifically,

$$\det(1 + \mathbf{S}[\delta]) = e^{\text{Tr} \ln(1 + \mathbf{S}[\delta])} \approx e^{\text{Tr} \mathbf{S}[\delta]}, \quad (63)$$

with the quadratic effective action for the scalar fluctuations as

$$\text{Tr} \mathbf{S}[\delta] = - \int \frac{d^3p}{(2\pi)^3} \delta(p) \mathbf{G}^{-1}(p) \delta(-p), \quad (64)$$

with to order $\mathcal{O}(\tilde{\alpha}^3)$

$$\begin{aligned} \mathbf{G}^{-1}(p) \approx & n_D + 4\tilde{\alpha}^2 M^8 \int \frac{d^3k}{(2\pi)^3} \\ & \times \left[\frac{k^4}{(k^2 + M^2)^4} \frac{1}{((k+p)^2 + M^2)^2} \right. \\ & \left. + \frac{2k^2}{(k^2 + M^2)^3} \frac{1}{((k+p)^2 + M^2)^2} \right]. \end{aligned} \quad (65)$$

The n_D contribution in (65) follows from the expansion of the leading contribution \mathcal{V} using arguments similar to those used for the derivation of the dyonic densities above.

The scalar structure factor follows from (65) through the normalization

$$\mathbf{G}_S(p) \equiv \frac{n_D}{V_3} \langle |\delta(p)|^2 \rangle = n_D \mathbf{G}(p). \quad (66)$$

We note that the small momentum fluctuations in δf couple to the soundlike modes. Specifically,

$$\mathbf{G}_S(p) \approx \frac{p^2}{c_s^2 p^2} \quad (67)$$

is dominated by a massless pole at zero momentum with

$$c_s^2 \approx 1 + 8\tilde{\alpha}^2 \left(\frac{M}{T} \right) \int \frac{d^3k}{(2\pi)^3} \left[\frac{k^4}{(k^2 + 1)^6} + \frac{2k^2}{(k^2 + 1)^5} \right]. \quad (68)$$

Alternatively, from the pressure (35) we expect

$$c_s^2 \equiv \frac{\partial \mathcal{P}_{\text{cl}}}{T \partial n_D} \approx 1 + \frac{\kappa(\tilde{\alpha})}{4\pi} \left(\frac{M}{T} \right), \quad (69)$$

with $\kappa(\tilde{\alpha}) \approx 15\tilde{\alpha}^2/32$ in leading order and in total agreement with (68). Also, at large momentum, Eq. (66) asymptotes $\mathbf{G}_S(\infty) = 1$. The slight superluminal character of (68) reflects on the fact that dyons are, in essence, Euclidean configurations with no physical particle realization.

G. Estimate of the critical T_c

The total thermodynamical pressure of the dyon-antidyon liquid consists of the classical and nonperturbative contribution (40) plus the perturbative holonomy potential known as the Gross-Pisarski-Yaffe-Weiss (GPYW) potential [17], plus the purely perturbative black-body

contribution (ignoring the higher-order $\mathcal{O}(\alpha_s)$ quantum corrections). Specifically, ($N_c = 2$):

$$\frac{\mathcal{P}_{\text{tot}}}{T^4} \approx \tilde{n}_D + \frac{\kappa(\tilde{\alpha})}{3\pi\sqrt{2}} \tilde{n}_D^{\frac{3}{2}} - \frac{\pi^2}{45} \left(N_c^2 - \frac{1}{N_c^2} \right) + \frac{\pi^2}{45} (N_c^2 - 1). \quad (70)$$

The Debye-Huckel contribution is of order N_c^3 , while the leading classical contribution is of order N_c^2 . So the screening and large N_c are not commutative. For the SU(2) case of interest, the transition temperature T_c from the disordered phase ($\nu = 1/2$) to the ordered phase ($\nu = 0$) occurs when the first three contributions in (70) cancel out. Thus,

$$\tilde{n}_D + \frac{\kappa(\tilde{\alpha})}{3\pi\sqrt{2}} \tilde{n}_D^{\frac{3}{2}} \approx \frac{\pi^2}{12}. \quad (71)$$

For $\kappa(-0.52) \approx 0.19$, the critical density is $n_D^c \approx \pi^2 T_c^3 / 12 \approx 0.88$. Since the SU(2) electric string tension is $\sigma_E = TM = \sqrt{2n_D T}$ (see below), it follows that $T_c / \sqrt{\sigma} = 6^{1/4} / \sqrt{\pi} \approx 0.88$ which is somehow larger than the SU(2) lattice result $T_c / \sqrt{\sigma_E} = 0.71$ [29].

IV. POLYAKOV LINES

To probe the confining nature of the dyon-antidyon liquid in the three-dimensional effective theory, we will compute explicitly the expectation of a heavy quark through the traced Polyakov line and the correlator of a heavy quark-antiquark pair through the correlator of the traced Polyakov line and its conjugate at fixed spatial separation. The insertion of these charges in the dyon-antidyon liquid modifies the ground state through solitonic solutions around these sources.

In this section we present a new derivation of the pertinent solitonic equations for the SU(2) case that makes explicit use of the presence of the long-range U(1) b and σ fields. In the linearized screening approximation, we show that the solitonic equations for the heavy source probes are in agreement with those established in [4] using different arguments.

A. $\langle L \rangle$

In the SU(2) case the Polyakov line consists of inserting a heavy quark whose free energy consists of its Coulomb interactions with all the Coulomb charged dyons and antidyons. Specifically, the traced Polyakov line before averaging is

$$L(x_1) = e^{2\pi i \mu_M + \frac{i}{2T} \sum_i \left(\frac{1}{|x_1 - x_{Mi}|} + \frac{1}{|x_1 - x_{\bar{M}i}|} - \frac{1}{|x_1 - x_{Li}|} - \frac{1}{|x_1 - x_{\bar{L}i}|} \right)} + e^{2\pi i \mu_L + \frac{i}{2T} \sum_i \left(\frac{1}{|x_1 - x_{Li}|} + \frac{1}{|x_1 - x_{\bar{L}i}|} - \frac{1}{|x_1 - x_{Mi}|} - \frac{1}{|x_1 - x_{\bar{M}i}|} \right)}, \quad (72)$$

with $\mu_L - \mu_M = v_m$. When averaging using the ensemble (2), it is clear that each of the contributors to the string of factors in (72) will match its analogue from the measure and reexponentiate. For instance, the first contribution in (72) reexponentiates through the substitution

$$e^{-b \pm i\sigma} \rightarrow e^{-b \pm i\sigma} e^{\frac{i}{2T|x_1 - x|}}. \quad (73)$$

The extra Coulomb factors can be redefined away by shifting

$$b \rightarrow b + \frac{i}{2T|x_1 - x|}, \quad (74)$$

thereby changing the constraint equation (25) to

$$\begin{aligned} & -\frac{T}{4\pi} \nabla^2 w_M + f(e^{w_M - w_L} - e^{w_L - w_M}) \\ & = \frac{T}{4\pi} \nabla^2 (b - i\sigma) + \frac{i}{2} \delta^3(x - x_1) \\ & -\frac{T}{4\pi} \nabla^2 w_L + f(e^{w_L - w_M} - e^{w_M - w_L}) = 0, \end{aligned} \quad (75)$$

and similarly for the second contribution in (72) with $L \leftrightarrow M$. The effect of the first contribution in the Polyakov line (72) is to add a source term to the constraint equation for w_M . It is in agreement with [4] after setting $b = \sigma = 0$. Equation (75) is a Poisson-Boltzmann-type equation. It is also referred to as an elliptic and periodic Toda lattice [4,30]. The solution is a local Debye-like cloud around the inserted heavy quark,

$$(w_M - w_L)(x) \approx \frac{2\pi i}{T} \int \frac{d^3 p}{(2\pi)^3} \frac{e^{ip \cdot (x - x_1)}}{p^2 + M^2}. \quad (76)$$

This causes almost no change in the vacuum holonomies $v_{m,L}$. Thus, after the shift

$$\langle L(x_1) \rangle \approx e^{i2\pi\mu_M} + e^{i2\pi\mu_L} = 0. \quad (77)$$

B. $\langle LL^\dagger \rangle$

The preceding analysis can also be applied to the correlator of two heavy quarks through LL^\dagger which consists now of four contributions before averaging

$$L(x_1)L^\dagger(x_2) = \sum_{m,n=M,L} e^{2\pi i(\mu_m - \mu_n)} e^{\frac{i}{2T}(F_m(x_1) - F_n(x_2))}, \quad (78)$$

with the pertinent Coulomb free energies $F_m(x_{1,2})$ following from (72). When averaged over the measure (3), each of the factors in (78) can be matched with its analogue in the measure. The preceding observations show that the Coulomb factors in the probing correlator can be paired with

$$e^{-b\pm i\sigma} \rightarrow e^{-b\pm i\sigma} e^{\frac{i}{2T|x-x_1|} - \frac{i}{2T|x-x_2|}}. \quad (79)$$

A rerun of the preceding arguments shows that the constraint equations now acquire two source contributions, one for each of the heavy quarks inserted:

$$\begin{aligned} & -\frac{T}{4\pi} \nabla^2 w_M + f(e^{w_M - w_L} - e^{w_L - w_M}) \\ & = \frac{T}{4\pi} \nabla^2 (b - i\sigma) + \frac{i}{2} [\delta^3(x - x_1) - \delta^3(x - x_2)] \\ & -\frac{T}{4\pi} \nabla^2 w_L + f(e^{w_L - w_M} - e^{w_M - w_L}) = 0. \end{aligned} \quad (80)$$

Since $\nabla^2 1/|x - x_2| = -4\pi\delta^3(x - x_2)$, we can symmetrize (80) by shifting $\delta^3(x - x_2)$ from the first to the second equation through

$$w_{M,L} \rightarrow w_{M,L} + \frac{i/T}{2|x - x_2|}, \quad (81)$$

with unit Jacobian. The symmetrized (80)–(81) equations are in agreement with those established in [4] for the SU(2) case after setting $b = \sigma = 0$. In this case the solution is peaked around the heavy quark sources:

$$(w_M - w_L)(x) \approx \frac{2\pi i}{T} \int \frac{d^3 p}{(2\pi)^3} \frac{e^{ip \cdot (x-x_1)} - e^{ip \cdot (x-x_2)}}{p^2 + M^2}. \quad (82)$$

Inserting this back in the expectation value of the correlator (78) yields asymptotically

$$\langle L(x_1) L^\dagger(x_2) \rangle \approx e^{-M|x_1 - x_2|} \quad (83)$$

in the three-dimensional effective theory in agreement with the result in [4]. In four dimensions, (83) translates to confinement of the electric charges with the electric string tension $\sigma_E = MT$. The additional Coulomb screening in (3) does not affect the asymptotics of the linearly rising heavy quark potential to leading order. The dyon-antidyon Coulomb liquid still electrically confines in the center symmetric phase.

V. SINGLE-WINDING WILSON LOOP

To study the large spatial Wilson loops, we use the same observations made above in the presence of the U(1) fields σ and b . As an observable, the traced spatial Wilson loop of area S supported by the spatial contour $\partial S = C$ reads

$$\text{Tr}W(C) = e^i \int_S B_+ \cdot dS + e^i \int_S B_- \cdot dS \quad (84)$$

and sources the static magnetic field

$$B_{\pm\mu} = \pm \sum_i Q_i \frac{(x - x_i)_\mu}{|x - x_i|^3}. \quad (85)$$

When averaged using (3), the spatial Wilson loop (84) modifies the additional U(1) fugacity factors in the dyon sector. Their contribution follows again by shifting $b \mp i\sigma \rightarrow b \mp i(\sigma - \eta_\pm)$ in the constraint equations with

$$\eta_\pm(x) = \pm \int_S dS_y \cdot \frac{x - y}{2|x - y|}. \quad (86)$$

As a result, Eqs. (25) in the presence of (84) are now modified to read

$$\begin{aligned} & -\frac{T}{4\pi} \nabla^2 w_M + f(e^{w_M - w_L} - e^{w_L - w_M}) = \frac{iT}{4\pi} \nabla^2 \eta_+(x) \\ & -\frac{T}{4\pi} \nabla^2 w_L + f(e^{w_L - w_M} - e^{w_M - w_L}) = 0 \end{aligned} \quad (87)$$

for the first contribution and similarly for the second contribution in (84) with $\eta_+ \rightarrow \eta_-$. After choosing the spatial Wilson loop to lay in the x - y plane through $\nabla^2 \eta_\pm = \pm 4\pi\delta'(z)$, the results (87) are in agreement with those derived in [4] for the SU(2) case but without the long range U(1) σ and b fields in the leading-order approximation. Thus $\langle \text{Tr}W(C) \rangle \approx e^{-\sigma_M S}$ is saturated by the pinned soliton, with the magnetic string tension $\sigma_M = \sigma_E = MT$. This result is expected from the equality of the electric and magnetic masses in (55).

A simple understanding of this result is as follows: while a heavy quark sources an electric field, a large spatial Wilson loop sources a magnetic field by Ampere's law which is classically composed of all the magnetic poles fluxing S as is explicit in (85). The typical contribution to (84) for a planar surface in the x - y plane is then

$$\langle e^i \int_S B \cdot dS \rangle \approx e^{-\frac{S}{2} \int_S \langle B_z(x,y) B_z(0,0) \rangle dS} \quad (88)$$

by keeping only the first cumulant in the average and using translational invariance for large S . In this limit, S acts as a uniformly charged magnetic sheet classically made of magnetic dyons, so that

$$\langle B_z(x,y) B_z(0,0) \rangle \approx \left\langle \left(\frac{Q_M}{S} \right)^2 \right\rangle \approx \frac{\langle Q_M \rangle}{S^2}, \quad (89)$$

where the variance in the magnetic charge is assumed Poissonian. The magnetic charge density per unit 4-volume is $(TM)^2/2$. The typical magnetic charge per unit area is then about its square root or $\langle Q_M \rangle/S \approx TM$. Thus,

$$\langle e^i \int_S B \cdot dS \rangle \approx e^{-\frac{1}{2} MTS}, \quad (90)$$

which is the expected behavior up to a factor of order one in the string tension.

VI. DOUBLE-WINDING WILSON LOOP

Recently it was pointed out in [31] that a coplanar and double winding Wilson loop in the SU(2) pure gauge theory version of the model discussed by Diakonov and Petrov [4] shows an exponential falloff with the sum of the areas. In contrast, lattice SU(2) simulations appear to show an exponential falloff with the difference of the areas. The main observation in [31] is that the solitonic configuration contributing to the single-winding spatial Wilson loop, as for instance from our linearized version with $b = \sigma = 0$ in (87), factors out in the double-winding and coplanar Wilson loop.

For two identical loops with $C_1 = C_2 = C$, we have the formal SU(2) identities [32] (and references therein):

$$\begin{aligned} (\text{Tr}W(C))^2 &= \text{Tr}_S(W(C)) + \text{Tr}_A(W(C)) \\ \text{Tr}(W(C)^2) &= \text{Tr}_S(W(C)) - \text{Tr}_A(W(C)). \end{aligned} \quad (91)$$

The simple trace Tr is carried over the fundamental representation of N-ality $k = 1$ as in (84), and $\text{Tr}_{S,A}$ are carried over the symmetric and antisymmetric of N-ality $k = 2$ (modulo 2) representations of SU(2), respectively. The identities (92) are commensurate with the Young-Tableau decomposition. In the dyonic plasma considered here, the k -string tensions σ_k in the linearized plasma approximation are identical to those derived in [4] with $\sigma_k/\sigma_1 = \sin k\pi/2$ for SU(2) with $\sigma_1 = \sigma_E$. For $k = 2$ we have $\sigma_2 = 0$ and the second identity in (92) implies for large loops

$$\langle \text{Tr}(W(C)^2) \rangle = \langle \text{Tr}_S(W(C)) \rangle - 1. \quad (92)$$

We have set all self-energies to zero for simplicity as they depend on the subtraction procedure. Equation (92) is consistent with the doubly traced Wilson loop as dominated by the $k = 2$ modulo 2 colorless di-quark-like (qq) or baryonlike configuration in SU(2). In the dyonic plasma, the double Wilson loop with $C_1 = C_2$ is a bound colorless state with zero size that is strongly correlated within the dyons cores and therefore is consistent with the arguments presented in [31].

For largely separated loops $C_{1,2}$ of arbitrary sizes but still lying in the spatial directions, clearly

$$\langle \text{Tr}(W(C_1)W(C_2)) \rangle \approx e^{-\sigma_E(A_1+A_2)} \quad (93)$$

for $(A_1 + A_2) < A_{12}$, where $A_{1,2}$ are the planar areas supported by $C_{1,2}$ separately, and A_{12} is the minimal area with boundaries C_1 and C_2 . The main issue is what happens for the same doubly wound SU(2) spatial Wilson loops when $A_{12} < (A_1 + A_2)$? Here we note that $L\vec{L}$ and $M\vec{M}$

dimers carrying $(-2, 0)$ and $(+2, 0)$ (electric, magnetic) charge assignments could cluster around the probe qq (baryon) and $\bar{q}\bar{q}$ (antibaryon) configurations, respectively, to form neutral molecular bound states with masses that scale with A_{12} instead of $(A_1 + A_2)$. They are commensurate with the massive off-diagonal and charged gluons Higgsed by the holonomy and dropped in the dyon liquid analysis. These configurations were not retained in [4].

VII. T' HOOFT LOOPS

In an important study of the nature of confinement in gauge theories, t' Hooft [33] has introduced the concept of a disorder operator or t' Hooft loop to quantify confinement in the Hilbert space of gauge configurations. The t' Hooft loop is a canonical operator much like the Wilson loop. In a Lorentz-invariant confining vacuum, t' Hooft has argued that the temporal Wilson loop and the t' Hooft loop cannot exhibit an area law simultaneously. The temporal Wilson loop obeys an area law, while the t' Hooft loop obeys a perimeter law.

Physically, the Wilson loop corresponds to a color charge in the fundamental representation running around a closed loop and measuring the the chromomagnetic flux across the loop. The t' Hooft loop corresponds to a dual charge in the center of the gauge group running around a closed loop and measuring the chromoelectric flux across the loop. The t' Hooft loop is the dual of the Wilson loop.

In the temperature range $0.5T_c < T < T_c$, confinement is still at work and we expect the temporal Wilson and t' Hooft loops to exhibit behaviors similar to those in the vacuum state. In Sec. V we have explicitly checked that the closed spatial Wilson loop obeys an area law. The temporal Wilson loop is not amenable to our dimensionally reduced and Euclideanized effective field theory.

The t' Hooft loop $V(C)$ enforces a gauge transformation Ω_C which is singular on a closed curve C . If a curve C' winds $n_{CC'}$ times around C then

$$V^\dagger(C)W(C')V(C) = e^{i\frac{2\pi}{N_c}n_{CC'}}W(C'). \quad (94)$$

$V(C)$ amounts to a multivalued gauge transformation on the loop C ,

$$\Omega_C(\theta = 2\pi) = e^{i\frac{2\pi}{N_c}n_{CC'}}\Omega_C(\theta = 0), \quad (95)$$

with θ an affine parameter along C . A simple choice is

$$\Omega_C(x) = e^{i\frac{2\pi}{N_c}Q\varphi_C(x)}, \quad (96)$$

where $\varphi_C(x)$ is a multivalued scalar potential for the magnetic field \vec{B}_C generated by a loop of current \vec{j}_C running along C , and $Q = (1, 1, \dots, -N_c + 1)$, a Cartan generator of SU(N_c). An alternative construction using

a discontinuous solid angle was discussed in [37,38]. The effects of (96) on an Abelianized Wilson loop is

$$\Omega_C^\dagger \left(e^{i \int_{C'} ds \cdot A} \right) \Omega_C = e^{i \int_{C'} ds \cdot (A - \frac{2\pi}{N_c} Q B_C)}, \quad (97)$$

with $\vec{B}_C = -\vec{\nabla} \varphi_C$. Note that since φ_C is multivalued, we have $\vec{\nabla} \times \vec{B}_C = 4\pi \vec{j}_C$. If we normalize the loop current \vec{j}_C such that

$$\int_{C'} ds \cdot B_C = 4\pi \int_{A(C')} dS \cdot j_C = -n_{CC'}, \quad (98)$$

then (97) reduces to

$$\Omega_C^\dagger \left(e^{i \int_{C'} ds \cdot A} \right) \Omega_C = e^{i \frac{2\pi}{N_c} n_{CC'}} e^{i \int_{C'} ds \cdot A}. \quad (99)$$

In the space of gauge configurations, the gauge transformation Ω_C is enforced through

$$V(C) = e^{i \frac{2\pi}{g N_c} \int d^3 x \text{Tr}(E_i D_i(Q\varphi_C))}. \quad (100)$$

For SU(2) we have

$$V(C) = e^{i \frac{2\pi}{g} \int d^3 x \vec{E}^3 \cdot \vec{B}_C} \rightarrow e^{-\frac{2\pi}{g} \int d^3 x \vec{E}^3 \cdot \vec{B}_C}, \quad (101)$$

where the latter substitution $E \rightarrow iE$ follows in Euclidean space. With this in mind, the expectation value of the t' Hooft loop in the dyonic ensemble involves a string of sources to be inserted in (10). In leading order,

$$\begin{aligned} V(C) &\rightarrow \prod_{i=1}^{N+\bar{N}} e^{\frac{2\pi}{g} \int d^3 x B_C \cdot \nabla \frac{Q E_i}{|x-x_i|}} \\ &= \prod_{i=1}^{N+\bar{N}} e^{-\frac{2\pi}{g} \int d^3 x \nabla \cdot B_C \frac{Q E_i}{|x-x_i|}} = 1. \end{aligned} \quad (102)$$

Thus $\langle V(C) \rangle = 1$ modulo $\mathcal{O}(\alpha_s)$ Coulomb-like self-energy corrections which are, in general, perimeterlike.

Finally, the Polyakov line as a Wilson loop around the periodic temporal direction has a dual Polyakov loop with a dual magnetic charge in the center. In the confined phase, the temporal component of the gauge field A_4 asymptotes fixed electric-type holonomies, while its dual \tilde{A}_4 asymptotes zero dual magnetic-type holonomies thanks to parity. A rerun of the arguments in Sec. IV A shows that while $\langle L(\mathbf{x}) \rangle = 0$ in (77) as expected in a Euclidean and confining thermal state, its dual does not vanish, i.e.,

$$\langle \tilde{L}(\mathbf{x}) \equiv \text{Tr} \left(e^{i \frac{4\pi}{g N_c} \int_0^\beta Q \tilde{A}_4^Q(x) d\tau} \right) \rangle = 1 \quad (103)$$

again modulo $\mathcal{O}(\alpha_s)$ Coulomb corrections. This behavior is consistent with the one reported on the lattice for $N_c = 2, 3$ [34].

VIII. CONCLUSIONS

The central theme in this paper is nonperturbative gauge theory for temperatures in the range $(0.5-1)T_c$ modeled by a dense plasma of instanton-dyons. The new element in our discussion is the introduction of the leading classical $\mathcal{O}(1/\alpha_s)$ interactions between the dyons and antidyons as recently obtained in [22] using the classical “streamline” set of configurations for $M\bar{M}, L\bar{L}$ pairs. We have assumed that the $M\bar{L}, L\bar{M}$ channels are repulsive and opposite in sign to the streamline interaction. While completing this work, this assumption has now been confirmed numerically [35]. Another important element of our analysis is the one-loop measure of the dyon and antidyon moduli space, in the form proposed by Diakonov and Petrov [4]. It leads to a small moduli space volume and, thus, repulsive interaction at higher density, which however can be made much less repulsive by introducing correlations between the charges.

On general grounds, an ensemble of instanton-dyons is a strongly coupled plasma, with significant correlations between the particles. Therefore, the statistical mechanics of a generic instanton-dyon ensemble is very nontrivial and remains unsolved. However—and this is the main argument of the paper—when the plasma is dense enough for temperatures below T_c , it generates a large screening mass M which screens the interaction. A standard weak coupling plasma theory, in a form similar to the Debye-Huckel theory, is then applicable. The dimensionless 3-density of each dyon species $n_D/4$ in the regime considered is in the range of $n_D/4 \approx T^3/4$, in agreement with the qualitative arguments in [19].

Using it, we get a number of results concerning the details of the nonperturbative gauge fields, in the temperature range $(0.5-1)T_c$. First, in the presence of strong screening the minimum of the free energy is still at the confining (center symmetric) value of $\nu = 1/2$, with a vanishing Polyakov line $\langle L \rangle \approx \cos(2\pi\nu) = 0$. Second, a resummation of the the linearized screening effects yields Debye-Huckel-type corrections to the pressure and dyonic densities. We have also analyzed the topological susceptibility, the gluonic compressibility, and the electric and magnetic gluonic condensates in this linearized approximation.

We have calculated also the electric and magnetic screening masses, generated by the dyon ensemble. We have found that the latter are larger than the former in the confined phase. This is qualitatively consistent with the existing lattice data, which however are much better measured for the SU(3) gauge theory rather than the SU(2) one we have studied here. Finally, we have calculated the structure factors in the electric and magnetic sector in the linearized screening approximation as well. For an estimate of the transition temperature from $\nu = 1/2$ (confinement) to $\nu = 0$ (deconfinement), we have switched the perturbative (GPYW) holonomy potential [17] in

Sec. III G. For SU(2) the transition is observed to take place at $T_c/\sqrt{\sigma_E} \approx 0.88$.

In the dyonic plasma the large spatial Wilson loops exhibit area law, while the spatial 't Hooft loops are found to be 1 modulo $\mathcal{O}(\alpha_s)$ Coulomb-like self-energy corrections. These dual behaviors were argued in [33] for confining gauge theories at zero temperature. We found them to hold in the confining dyon ensemble in the regime $0.5 < T < T_c$.

Needless to say, all these predictions can and should be confronted with the lattice data in the corresponding temperature range.

Finally, let us speculate about the dyon ensemble beyond the validity domain of the Debye-Huckel approximation. First of all, strongly coupled Coulomb plasmas are tractable by certain analytic and/or numerical (molecular dynamics) methods, see Refs [23,24] for similar development. Another option is to use brute force numerical simulations of the dyon ensemble [36]. Qualitatively, sufficiently strongly coupled plasmas develop either (i) correlations between particles, resembling a liquid with crystal-like correlations (“molten salt”) or (ii) particular neutral clusters, the simplest of which can be the LM instantons themselves or $L\bar{M}\bar{L}\bar{M}$ “instanton molecules.” Recent

(unquenched) lattice simulations indicate that the instantons and anti-instantons recombine into topologically neutral molecules across the transition temperature [39,40]. At much higher temperature, the perturbative gluons dwarf all classical gauge configurations forcing the holonomy to zero.

One obvious extension of this work should be into the large number of colors N_c . Strong correlations can appear, since $\Gamma_{D\bar{D}} \approx 1/\alpha_s \approx N_c \gg 1$. A similar mechanism, leading to crystallization, appears to take place in dense holographic matter where the baryons as instantons in the holographic direction split into a pair of dyons and rearrange in salt crystals [41].

Another obvious extension of this work is to include fermions, which we turn to in the second paper of the series [42].

ACKNOWLEDGMENTS

We would like to thank Jeff Greensite, Tin Sulejmanpasic, Mithat Unsal, and Ariel Zhitnitsky for their comments on the manuscript after it was posted. This work was supported by the U.S. Department of Energy under Contract No. DE-FG-88ER40388.

-
- [1] T. Schafer and E. V. Shuryak, *Rev. Mod. Phys.* **70**, 323 (1998); D. Diakonov, *Prog. Part. Nucl. Phys.* **51**, 173 (2003); M. A. Nowak, M. Rho, and I. Zahed, *Chiral Nuclear Dynamics* (World Scientific, Singapore, 1996).
- [2] N. I. Kochelev, *Phys. Lett. B* **426**, 149 (1998); D. Ostrovsky and E. Shuryak, *Phys. Rev. D* **71**, 014037 (2005); Y. Qian and I. Zahed, *Phys. Rev. D* **86**, 014033 (2012); **86**, 059902 (E) (2012); Y. Qian and I. Zahed, *Phys. Rev. D* **90**, 114012 (2014).
- [3] T. C. Kraan and P. van Baal, *Nucl. Phys.* **B533**, 627 (1998); T. C. Kraan and P. van Baal, *Phys. Lett. B* **435**, 389 (1998); K. M. Lee and C. h. Lu, *Phys. Rev. D* **58**, 025011 (1998).
- [4] D. Diakonov and V. Petrov, *Phys. Rev. D* **76**, 056001 (2007); D. Diakonov and V. Petrov, *Phys. Rev. D* **76**, 056001 (2007); D. Diakonov and V. Petrov, *AIP Conf. Proc.* **1343**, 69 (2011); D. Diakonov, arXiv:1012.2296.
- [5] D. Diakonov, N. Gromov, V. Petrov, and S. Slizovskiy, *Phys. Rev. D* **70**, 036003 (2004).
- [6] A. R. Zhitnitsky, arXiv:hep-ph/0601057; S. Jaimungal and A. R. Zhitnitsky, arXiv:hep-ph/9905540; A. Parnachev and A. R. Zhitnitsky, *Phys. Rev. D* **78**, 125002 (2008); A. R. Zhitnitsky, *Nucl. Phys.* **A921**, 1 (2014).
- [7] V. A. Fateev, I. V. Frolov, and A. S. Shvarts, *Nucl. Phys.* **B154**, 1 (1979); B. Berg and M. Luscher, *Commun. Math. Phys.* **69**, 57 (1979).
- [8] B. Martemyanov, S. Molodtsov, Y. Simonov, and A. Veselov, *Pis'ma Zh. Eksp. Teor. Fiz.* **62**, 679 (1995) [JETP Lett. **62**, 695 (1995)]; B. V. Martemyanov, S. V. Molodtsov, Y. A. Simonov, and A. I. Veselov, *Yad. Fiz.* **60**, 565 (1997) [*Phys. At. Nucl.* **60**, 490 (1997)]; Y. A. Simonov, *Proc. Int. Sch. Phys. “Enrico Fermi”* **130**, 319 (1996); A. Gonzalez-Arroyo and Y. A. Simonov, *Nucl. Phys.* **B460**, 429 (1996).
- [9] G. 't Hooft, *Nucl. Phys.* **B138**, 1 (1978).
- [10] S. Mandelstam, *Phys. Rev. D* **19**, 2391 (1979).
- [11] N. Seiberg and E. Witten, *Nucl. Phys.* **B426**, 19 (1994); **430**, 485(E) (1994).
- [12] A. M. Polyakov, *Phys. Lett. B* **59**, 82 (1975); *Nucl. Phys.* **B120**, 429 (1977).
- [13] M. Unsal and L. G. Yaffe, *Phys. Rev. D* **78**, 065035 (2008); M. Unsal, *Phys. Rev. D* **80**, 065001 (2009).
- [14] T. H. Hansson, H. B. Nielsen, and I. Zahed, *Nucl. Phys.* **B451**, 162 (1995).
- [15] E. Poppitz, T. Schfer, and M. Unsal, *J. High Energy Phys.* **10** (2012) 115; E. Poppitz and M. Unsal, *J. High Energy Phys.* **07** (2011) 082.
- [16] E. Poppitz, T. Schfer, and M. Unsal, *J. High Energy Phys.* **03** (2013) 087.
- [17] D. J. Gross, R. D. Pisarski, and L. G. Yaffe, *Rev. Mod. Phys.* **53**, 43 (1981); N. Weiss, *Phys. Rev. D* **25**, 2667 (1982).
- [18] E. Shuryak and T. Sulejmanpasic, *Phys. Lett. B* **726**, 257 (2013).
- [19] E. Shuryak and T. Sulejmanpasic, *Phys. Rev. D* **86**, 036001 (2012).

- [20] P. Faccioli and E. Shuryak, *Phys. Rev. D* **87**, 074009 (2013).
- [21] F. Bruckmann, S. Dinter, E. M. Ilgenfritz, M. Muller-Preussker, and M. Wagner, *Phys. Rev. D* **79**, 116007 (2009); F. Bruckmann, S. Dinter, E. M. Ilgenfritz, B. Maier, M. Muller-Preussker, and M. Wagner, *Phys. Rev. D* **85**, 034502 (2012).
- [22] R. N. Larsen and E. Shuryak, [arXiv:1408.6563](https://arxiv.org/abs/1408.6563).
- [23] B. A. Gelman, E. V. Shuryak, and I. Zahed, *Phys. Rev. C* **74**, 044909 (2006); S. Cho and I. Zahed, *Phys. Rev. C* **79**, 044911 (2009); S. Cho and I. Zahed, *Phys. Rev. C* **80**, 014906 (2009).
- [24] S. Cho and I. Zahed, *Phys. Rev. C* **82**, 054907 (2010); **82**, 044905 (2010); V. S. Filinov, Y. B. Ivanov, V. E. Fortov, M. Bonitz, and P. R. Levashov, *Phys. Rev. C* **87**, 035207 (2013); V. S. Filinov, Y. B. Ivanov, M. Bonitz, V. E. Fortov, and P. R. Levashov, *Phys. Lett. A* **376**, 1096 (2012); V. S. Filinov, Y. B. Ivanov, M. Bonitz, P. R. Levashov, and V. E. Fortov, *Phys. At. Nucl.* **74**, 1364 (2011).
- [25] C. Adami, T. Hatsuda, and I. Zahed, *Phys. Rev. D* **43**, 921 (1991).
- [26] M. Fisher and Y. Levin, *Phys. Rev. Lett.* **71**, 3826 (1993) and references therein.
- [27] V. G. Bornyakov and V. K. Mitrjushkin, *Phys. Rev. D* **84**, 094503 (2011).
- [28] O. Kaczmarek, F. Karsch, F. Zantow, and P. Petreczky, *Phys. Rev. D* **70**, 074505 (2004); **72**, 059903(E) (2005).
- [29] B. Lucini, M. Teper, and U. Wenger, *J. High Energy Phys.* **02** (2005) 033.
- [30] T. J. Hollowood, [arXiv:hep-th/9110010](https://arxiv.org/abs/hep-th/9110010).
- [31] J. Greensite and R. Hollwieser, *Phys. Rev. D* **91**, 054509 (2015).
- [32] J. Greensite, B. Lucini, and A. Patella, *Phys. Rev. D* **83**, 125019 (2011).
- [33] G. 't Hooft, *Nucl. Phys.* **B138**, 1 (1978).
- [34] L. Del Debbio, A. Di Giacomo, and B. Lucini, *Nucl. Phys.* **B594**, 287 (2001); *Phys. Lett. B* **500**, 326 (2001).
- [35] R. N. Larsen (private communication).
- [36] R. Larsen and E. Shuryak, [arXiv:1504.03341](https://arxiv.org/abs/1504.03341).
- [37] C. Korthals-Altes, A. Kovner, and M. A. Stephanov, *Phys. Lett. B* **469**, 205 (1999).
- [38] H. Reinhardt, *Phys. Lett. B* **557**, 317 (2003).
- [39] S. Sharma, V. Dick, F. Karsch, E. Laermann, and S. Mukherjee, *Proc. Sci.*, LATTICE (2014) 164.
- [40] E. V. Shuryak, *Phys. Lett. B* **196**, 373 (1987); T. Schaefer, E. V. Shuryak, and J. J. M. Verbaarschot, *Phys. Rev. D* **51**, 1267 (1995).
- [41] M. Rho, S. J. Sin, and I. Zahed, *Phys. Lett. B* **689**, 23 (2010); V. Kaplunovsky and J. Sonnenschein, *J. High Energy Phys.* **04** (2014) 022; S. Bolognesi and P. Sutcliffe, *J. Phys. A* **47**, 135401 (2014).
- [42] Y. Liu, E. Shuryak, and I. Zahed, *Phys. Rev. D* **92**, 085007 (2015).